Hydrologic Regime and Soil Property Interactions in a Drained Peatland

Clayton S. Word

Thesis submitted to the faculty of the Virginia Polytechnic Institute and State University in partial fulfillment of the requirements for the degree of

Master of Science
in
Forest Resources and Environmental Conservation

Daniel L. McLaughlin, Co-Chair
Brian D. Strahm, Co-Chair
Ryan D. Stewart
J. Morgan Varner

April 14th, 2020
Blacksburg, VA

Keywords: peatland, hydrology, soil properties, hydrologic restoration, Great Dismal Swamp

Hydrologic Regime and Soil Property Interactions in a Drained Peatland

Clayton S. Word

ABSTRACT

Globally, peatlands are vulnerable to degradation via drainage, with consequences for ecosystem structure and function such as increased fire vulnerability, soil oxidation, and altered vegetation composition. Peatland function is largely dependent on hydrologic regimes and their influences on the accumulation and properties of peat soil. Therefore, an understanding of soil-hydrology interactions is needed to inform management in drained peatlands, including expansive systems such as the Great Dismal Swamp (GDS; Virginia and North Carolina, USA) where hydrologic restoration is underway. Two physically distinct soil layers have been observed at GDS, the upper layer thought to be a result of past drainage and the lower layer more representative of an undisturbed state. To understand the occurrence and consequences of these distinct layers, we integrated continuous water level data, peat profile characterization, and analyzed soil physical and hydraulic properties. The transition from upper to lower peat soil layers typically occurred at depths below contemporary water level observations, suggesting that the upper layer may be a result of historical drainage with limited recovery following hydrologic restoration. We also found distinct differences between the properties of the two layers, where upper layers had lower fiber and organic matter contents and higher bulk densities. Further, upper layers had higher proportions of macropores, resulting in an overall lower water retention capacity. These differences in layer properties suggest the upper layer is more susceptible to drying, increasing fire vulnerability, oxidation, and shifts in vegetation composition that do not support current management objectives.

Hydrologic Regime and Soil Property Interactions in a Drained Peatland

Clayton S. Word

GENERAL AUDIENCE ABSTRACT

Peatlands provide many valuable ecosystem services, including carbon storage, water quality maintenance, and habitat provision. However, peatlands have been subjected to centuries of drainage (i.e., lowered water levels) to support timber harvesting, land conversion, and other land use actions. Drainage and the resulting drier conditions can lead to soil carbon loss, increased fire vulnerability, and changes in vegetation communities. Additionally, peatland drainage has consequences for peat soil properties and their role in ecosystem services. In an effort to restore peatland ecosystem services, hydrologic restoration, usually in the form of water control structures, is often implemented to reduce drainage and reestablish historical water levels. To guide restoration practices, research is needed to understand how drained peat soils respond to such hydrologic management. In this study, we investigated peat soil profiles, current water level regimes, and soil properties at the Great Dismal Swamp (Virginia and North Carolina, USA), a drained peatland currently undergoing hydrologic restoration. We found a visibly distinct upper soil layer, which we suggest developed as a result of past drainage and with little recovery under restored, wetter conditions. We also found that this upper layer has altered soil properties and thus is more vulnerable to drying, with implications for ecosystem function such as fire vulnerability, carbon sequestration and vegetation composition. Together, our findings will help inform restoration and water level management at GDS and our understanding of drained peatlands more broadly.

ACKNOWLEDGEMENTS

I would like to express my sincere gratitude for all the help and support I have received on this project. First, I would like to thank my advisors, Brian Strahm and Daniel McLaughlin, whose constant time, support and guidance has helped develop my skills as a scientist, and made this entire experience an enjoyable one. I would also like to thank my committee members, Ryan Stewart and Morgan Varner, for their support and guidance. Thanks to the staff at the Great Dismal Swamp, Fred Wurster, Karen Balentine and Chris Lowie, for their knowledge and support throughout the duration of the project. Thanks to Dave Mitchem, Tal Roberts, and Brandon Lester for their lab and technical support. To all those who assisted me in the field, Brooke Bass, Daniel Franz, and Gavin Washburn, your positive attitudes, moral support and willingness to trudge through a sincerely dismal environment made conducting fieldwork an unforgettable experience. To Trevor Amestoy, whose excellent work in the lab and field contributed greatly to the success of this project. And lastly, to my lab mates, Amanda Penino, Stephanie Duston, Jake Diamond, Gracie Erwin, and Tommy Cianciolo, thank you for the unconditional support in and out of the classroom, and making this entire experience a truly great time.

TABLE OF CONTENTS

LIST OF FIGURES

LIST OF TABLES

1. Introduction

1.1 Peatlands: Extent and Function

Peatlands are a type of wetland system characterized by their deep organic soils, having by definition greater than 30% organic matter and an organic surface layer at least 40 cm deep (Joosten and Clark, 2002; Soil Survey Staff, 2014). Peatlands vary in their classification depending on hydrology, species composition, and degree of decomposition (Bridgham et al., 1996). In the U.S. system of soil taxonomy, peat soils are classified as Histosols and further categorized based upon their fiber content, such that fibric soils (peats) have > 67% fiber content, hemic soils (mucky peats) have 33% - 67% fiber content, and sapric soils (mucks) have < 33% fiber content (ASTM, 2013; Soil Survey Staff, 2014; Kolka et al., 2016; Vasilas et al., 2017). Peatlands are the most prevalent wetland type in the world, making up 50-70% of all wetlands (Joosten and Clark, 2002). They exist across large latitudinal gradients, with approximately 80% of the world's peatlands located in boreal regions, 15-20% located in the tropics, and less than 5% in temperate regions (Lappalainen, 1996; Rein et al., 2008). Peatlands occupy only 3%, or 4 million km^2, of the Earth's land surface (Joosten and Clark 2002; Xu et al., 2018) but disproportionately contribute to terrestrial ecosystem services.

Peatlands provide a suite of ecosystem services including carbon sequestration and storage, water quality and storage, and habitat for unique flora and fauna (Joosten and Clark, 2002). For example, peat soils are responsible for one-third of all terrestrial soil carbon (Yu et al., 2010; Page et al., 2011; Turetsky et al., 2014), or approximately equal to that of carbon in the atmosphere (Ciasis et al., 2013). Additionally, peatland soils play important roles in water quality maintenance (e.g., through elemental storage and removal; Martin-Ortega et al., 2014) and in flood mitigation and regulation (Bonn et al., 2016). Moreover, the unique conditions of peat soils (e.g., water-logged, acidic, and nutrient poor) select for highly specialized organisms, increasing global biodiversity (Minayeva et al., 2016). Such peatland functions are largely dependent on peat soil profiles and properties that develop with persistent soil saturation (Clymo, 1984; Belyea and Clymo, 2001).

1.2 Peat Soil Properties

Peat formation is a defining and functionally important characteristic of peatland systems that is driven by soil moisture dynamics and, in turn, influences hydrologic and carbon cycles. Peat is formed when organic matter inputs exceed the rate of decomposition, as is common in anerobic wetland soils (Belyea and Clymo, 2001; Mitsch and Gosselink, 2007). The rate of decomposition within the soil profile is thus largely controlled by water table and associated soil moisture regimes (Clymo, 1984). The degree of decomposition further serves to influence peat soil physical properties (e.g., bulk density, fiber content, pore structure) with documented feedbacks to site hydrology and soil moisture dynamics (Boelter, 1968; Belyea and Clymo, 2001; Verry et al., 2011).

There are also depth-dependent differences in physical and hydraulic properties along the soil profile that relate to age and degree of decomposition (Fig. 1). That is, organic matter deposits that occur above the water table experience more frequent aerobic conditions, and thus have higher decomposition rates, yet are less decomposed than deeper layers due to age (Clymo et al., 1998). As a consequence, the degree of peat decomposition and thus bulk density typically increase with depth (Boelter, 1968; Clymo, 1984); whereas total porosity, macroporosity, and fiber content have been shown to decrease with depth (Boelter, 1968; Verry et al., 2011). With these gradients in physical properties, there are often coincident gradients in important hydraulic properties, such as decreases in hydraulic conductivity and increases in moisture retention with depth (Boelter, 1968, Verry et al., 2011). The combined effects of these properties have reciprocal feedbacks to soil moisture regimes and thus vegetation communities (Joosten and Clark, 2002), carbon sequestration rates (Clymo et al., 1998), and vulnerability to peat-consuming fires (Turetsky et al., 2014). However, peatlands are commonly degraded via drainage, a widespread disturbance that has consequences for peat soil properties and resulting ecosystem functions (Holden et al., 2006), calling for both research and restoration efforts focused on the interactions among hydrologic regimes and soil properties within drained peatlands.

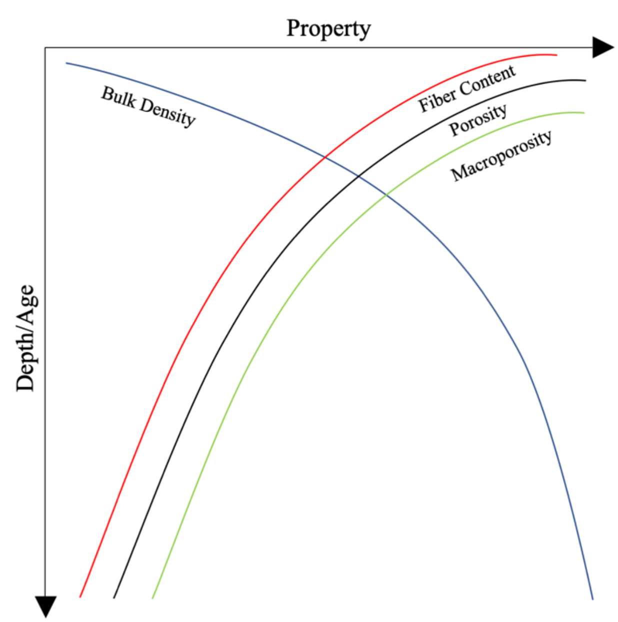

Figure 1: Conceptual model of peat soil properties associated with depth, age, and degree of decomposition. With increasing depth, and thus degree of decomposition, fiber content decreases and bulk density increases, which in turn affect moisture retention properties such as porosity and pore size distribution (macroporosity).

1.3 Peatland Disturbance

Globally, peatlands have lost approximately 486,000 km^2 of their land area since 1800, which represents a decrease of 11% in total area (Yu et al., 2010; Kolka et al., 2016). The primary mode of peatland degradation is through hydrologic alteration via drainage (Gorham and Rochefort, 2003), where ditch features are commonly used to facilitate forestry, road construction, and peat harvesting operations (Turetsky and Louis, 2006). The resulting lowered water tables have documented impacts on biogeochemical processes, fire vulnerability, and vegetation communities (Joosten and Clark, 2002: Turetsky and Louis, 2006). The consequence of soil oxidation on carbon storage is widely recognized, with estimates of carbon loss in disturbed peatlands ranging from to 0.25 – 26 t CO_2-C ha^{-1} yr^{-1} (IPCC, 2014). Additionally, reduced soil moisture in drained peatlands has increased the frequency and extent of smoldering fires (Turetsky et al., 2014), which can further release large amounts of carbon (Page et al., 2011) and be extremely difficult to extinguish (Rein et al., 2008). Last, lowered water tables can favor facultative over obligate wetland species, especially during forest regeneration, degrading overall vegetation composition (Atkinson et al., 2003).

1.4 Disturbance Effects on Peat Properties

More frequent aerobic conditions from drainage can lead to increased peat soil oxidation, which initiates a cascade of changes in peat soil properties, particularly in upper soil layers. Specifically, increased oxidation often leads to increased bulk density, decreased fiber content, and decreased pore volume (Kechavarzi et al., 2010; Leifeld et al., 2011). Undisturbed upper peat layers experience more frequent aerobic conditions and thus higher decomposition rates compared to lower layers, but depth differences in age and thus degree of decomposition typically result in the profile depicted in Figure 1 (i.e., lower bulk density in upper layers; Boelter, 1968; Clymo, 1984). Drainage and even further increases in oxidation may alter this general depth-dependent profile, such as increasing bulk density in upper layers (Kechavarzi et al., 2010).

Drainage and more frequent soil drying have also been shown to cause peat shrinkage, which can further affect upper soil properties including permanent changes to soil structure and associated moisture retention properties (Päivänen, 1982; Schwärtzel et al., 2002). Peat soil shrinkage and residual swelling are normal in peatlands and known as "mire breathing" (Schwärtzel et al., 2002). However, drying-induced shrinkage can become irreversible when peats are exposed to long-term and intensive drainage events (Schwärtzel et al., 2002; Peng et al., 2007; Gebhardt et al., 2009). This soil shrinkage can lead to distinguishable changes in pore structure in upper peat layers (Schwärtzel et al., 2002; Verry et al., 2011), the magnitude and depth of which are determined by factors such as degree of decomposition and antecedent water content (Päivänen, 1982). The resulting altered pore structure can have important consequences for water retention properties (Schwärtzel et al., 2002, Peng et al., 2007; Peng and Horn, 2007). Specifically, shrinkage can increase macroporosity, which in turn reduces capillary rise and increases hydraulic conductivity, while decreasing overall moisture retention (Wallor et al., 2018). These changes in pore structure and drying-induced hydrophobicity limit the recovery of peat soil structure with rewetting (Dekker and Ritsema, 1996; Peng et al., 2007; Peng and Horn, 2007). Consequently, peatland drainage can lead to persistent changes in physical and hydraulic peat properties, further affecting long-term soil moisture regimes and associated ecosystem functions.

1.5 Peatland Restoration

Globally, drained peatlands are undergoing restoration practices to reestablish historical hydrologic regimes in an effort to restore desired ecosystem properties and functions. Hydrology is often restored through the installation of water control structures in ditches, ditch filling, or plugging of other drainage features (Chimmer et al. 2016). A common goal of reestablishing previous hydrologic regimes is for peat-forming species, like *Sphagnum* and *Carex* spp., to recolonize and support peat soil accumulation (Gorham and Rochefort, 2003). Water levels are also managed to enhance regeneration of other obligate wetlands species and to reduce fire vulnerability (Chimmer et al. 2016). However, potential and irreversible changes in water retention properties of degraded peat soils represents an important, and largely unrecognized, challenge for such restoration efforts. Thus, an improved understanding of the occurrence and consequences of degraded peat soil properties is needed to effectively manage and restore drained peatland systems.

1.6 Objectives

Here, we examine interactions between hydrologic regimes and soil properties in the Great Dismal Swamp National Wildlife Refuge (GDS), an intensively drained forested peatland system located in southeastern Virginia and northeastern North Carolina, USA. Specific objectives include:

1. Relate thickness of the upper peat soil layer with long-term water levels.
2. Contrast the physical and hydraulic properties of upper and lower peat soil layers.

2. Materials and Methods

2.1 Study Site

This study took place in the Great Dismal Swamp National Wildlife Refuge (GDS), a drained, forested peatland currently undergoing hydrologic restoration under the management of the U.S. Fish and Wildlife Service. GDS is located on the border of southeastern Virginia and northeastern North Carolina (36.6201, -76.5599). Climate at GDS is temperate, characterized by long humid summers and mild winters. Mean annual precipitation is 128 cm, and mean annual temperature is 16°C (1981-2018; PRISM Climate Group). GDS has deep, organic-rich soils mapped as Typic Haplosaprists (Soil Survey Staff, 2020) but is typically described as a peatland (e.g., Atkinson et al., 2003; Eggleston et al., 2018) following general peatland definitions as wetland systems with deep (> 40 cm) Histosols (Joosten and Clark, 2002; Kolka et al., 2016).

GDS once extended over more than contiguous 500,000 ha (Osborn, 1919), characterized by peat depths greater than 4 m and dominated by stands of Atlantic white-cedar (*Chamaecyparis thyoides*), bald-cypress (*Taxodium distichum*), black gum (*Nyssa sylvatica*), and swamp tupelo (*Nyssa biflora*) (Whitehead, 1972; Levy, 1991). Beginning in the mid-18th century, ditches were installed across GDS to lower water tables and accommodate timber harvesting (Levy, 1991). The lowered water tables resulted in an increase in aerobic conditions, increasing peat soil oxidation and subsidence (USFWS, 2006; Chimmer et al., 2016). Further, lower soil moisture regimes are thought to be responsible for the now widespread dominance of red maple (*Acer rubrum*; Whitehead, 1972) and loss of obligate wetland species (e.g., bald-cypress, Atlantic white-cedar; Atkinson et al., 2003). Lastly, drier conditions have increased vulnerability to smoldering fire, including two recent wildfires that burned up to 1 m depth of peat and released approximately 1.70 Tg of carbon to the atmosphere (Sleeter et al., 2017).

In 1973, GDS became a National Fish and Wildlife Refuge (NFWR), and has since been preserved and managed for habitat and carbon storage functions. Today, GDS occupies 45,000 ha and includes a 240 km ditch network (Atkinson et al., 2003; Eggleston et al., 2018) from over two centuries of drainage. Since becoming a NFWR, water control structures have been installed throughout this ditch network to raise water levels, with the goals of increased carbon sequestration, biodiversity, and reduced fire vulnerability (Wurster et al., 2016). Due to historical drainage, however, GDS soils have likely been altered and are now characterized by two distinct layers, an upper peat soil layer (hereafter referred to as upper layer) that has a weak subangular blocky structure, and a lower peat soil layer (hereafter referred to as lower lower) that that is more massive and sapric (Soil Survey Staff, 2020) (Fig. 2).

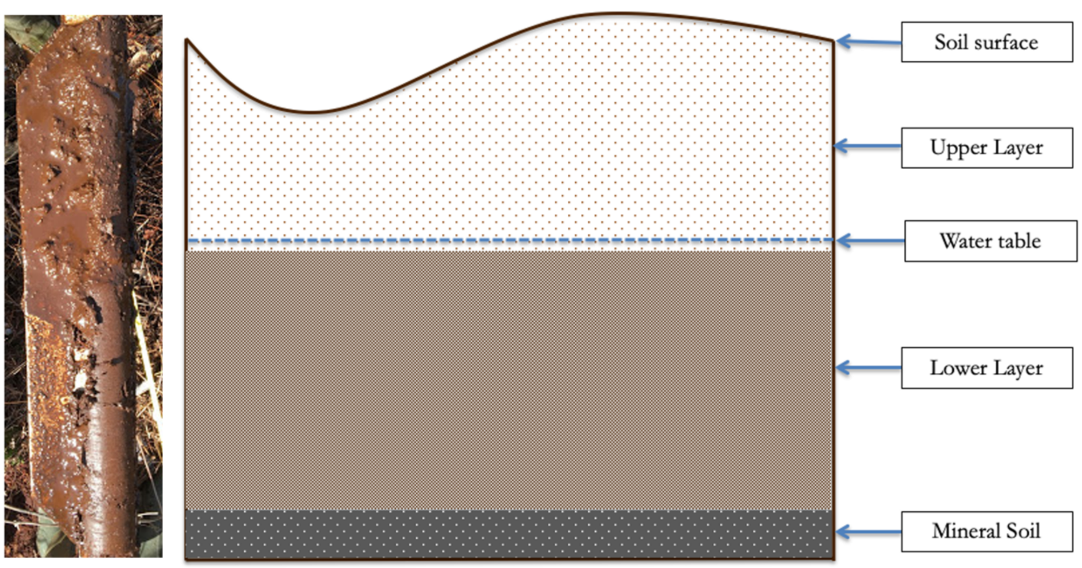

Figure 2: Left, 50-cm soil core taken from GDS, highlighting both upper (subangular blocky structure) and lower (massive structure) peat layers. Right, conceptual schematic of peat layers at GDS with an upper layer, thought to be an artifact of historical drainage, and a lower layer, thought to be less disturbed, underlain by mineral substrate. The location of the water table fluctuates throughout the profile.

2.2 Plot Selection and Layout

To evaluate spatial variation in soil layer depths, water table dynamics, and soil physical and hydraulic properties within GDS, we established 16 plots (Fig. 3), co-located with existing water table monitoring wells (managed by GDS staff). Plots were selected under the following criteria: they existed on peat deposits; had overlapping water level data of at least 2.5 years; and had no changes to water level management over that time period (i.e., no changes to water control structures near that plot that would change contemporary hydrologic regime). Each plot consisted of three subplots, each located 8 m from the well (plot center) on azimuths of 0°, 120° and 240°. If a subplot location fell on any obstruction (e.g., tree, cypress knees, roots), the transects were rotated 10° clockwise until there were no longer any obstructions.

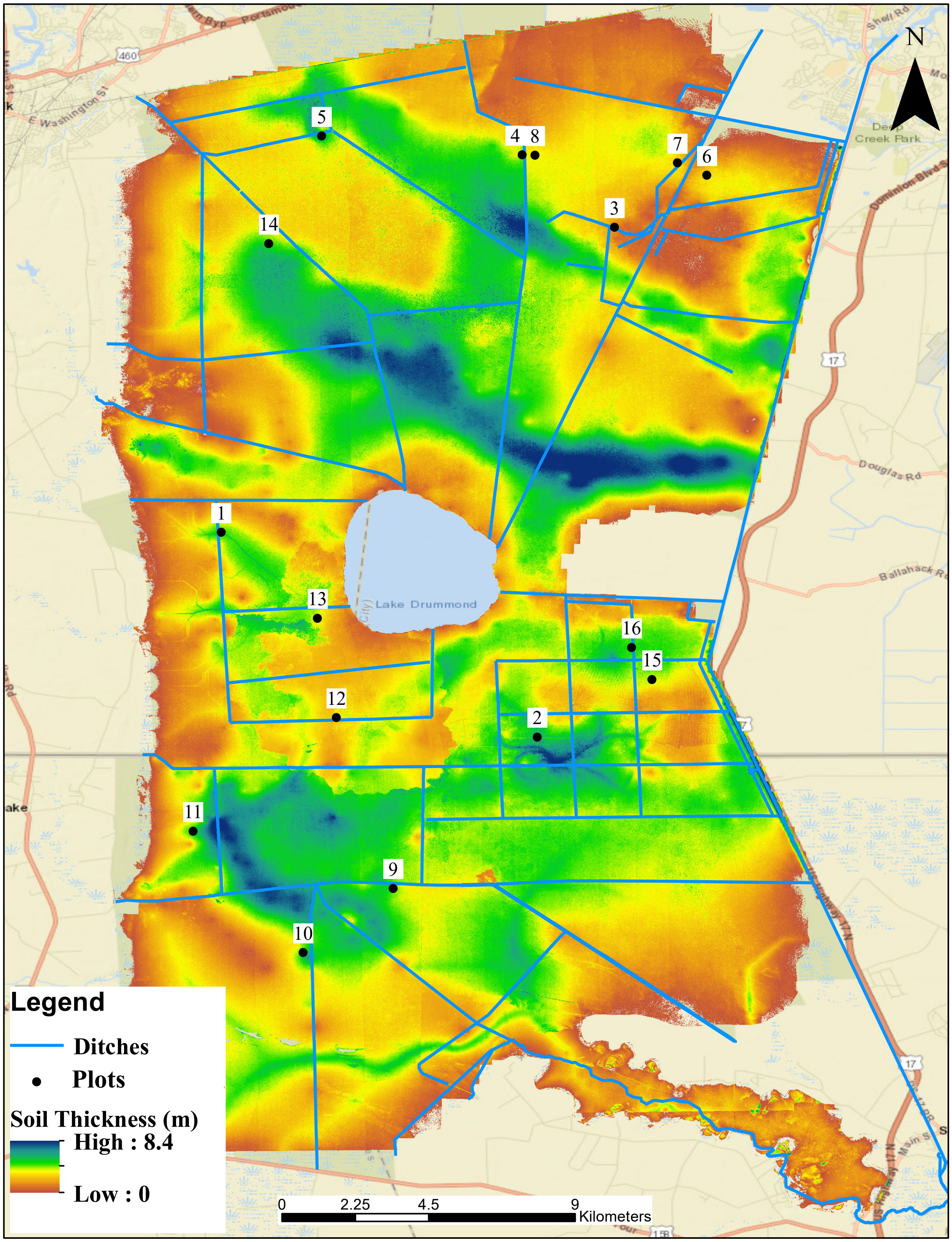

Figure 3: Map of organic soil thickness, plot locations, and ditch networks at the Great Dismal Swamp National Wildlife Refuge.

2.3 Objective 1: Relating Soil Profiles to Hydrologic Regime

2.3.1 Soil Profile Characterization

At each subplot, total peat soil depth, layer depth and thickness, and water table depth from ground surface were measured. Total peat soil depth was measured using a soil rod (Fig. 4A), pushed by hand until refusal by the underlying mineral layer. Individual layer depths and thicknesses were measured using intact cores from a Russian Sediment/Peat Borer (AMS, Inc., American Falls, Idaho, USA) (Fig. 4B). The Russian peat borer takes 50 cm long intact cores, which were extracted sequentially until all organic layers were represented. Layers were identified in the field by qualitative characteristics, where upper layers were characterized by coarse, sub-angular blocky structure and lower layers exhibited a massive muck structure, more typical of undisturbed Haplosaprists (Figure 2; Soil Survey Staff, 2020). Each layer was then measured for depth and thickness.

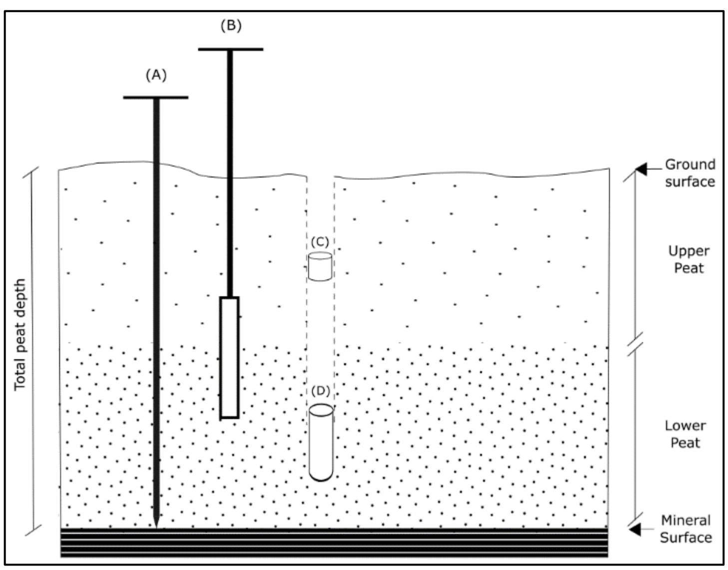

Figure 4: Subplot soil profile characterization (all subplots) and sampling (one subplot per plot) including: (A) soil rod for total organic soil depth, (B) Russian peat borer used to characterize upper and lower soil layers, (C) 5 cm × 5 cm bulk density sampler ring for upper soil layer sampling, and (D) 5 cm × 25 cm hand core sediment sampler tube for lower soil sampling. Used with permission from Trevor Amestoy, Research Undergraduate Fellow, Virginia Tech Institute for Critical Technology and Applied Science.

2.3.2 Water Table Regime Characterization

Sub-daily (30 minute) water table data (March 2017 to September 2019) at each plot center were obtained from either the USGS National Water Information System (U.S. Geological Survey, 2016) or GDS staff, depending on well ownership. To estimate water table depth regimes at each subplot, we surveyed each subplot's ground surface elevation relative to ground surface at the well (i.e., plot center). To do so, a clear rubber hose (0.85 cm in diameter) filled with water was used as a manometer (FAO, 1985). We then calculated water table depths based on the difference between the surface elevations at each subplot and the water elevations at the plot center, assuming a locally flat water table. To validate the assumption of a flat water table, we compared differences between subplot and plot center water table depths observed at time of soil characterization versus their surveyed elevation differences, which resulted in a significant linear relationship ($R^2 = 0.86$, $p < 0.001$) with a slope of 0.94. We then used the water table depth data to determine several metrics for each subplot, including mean, median, standard deviation, 25th, 75th and 95th percentiles, and cumulative density functions (CDF).

2.3.3 Relationships Between Upper Layer Thickness and Water Table Metrics

To relate soil profiles to hydrologic regimes, we conducted a Spearman's correlation (α = 0.05) between observed upper layer thicknesses and the suite of water table depth metrics, where data were checked for normality using the Shapiro-Wilk normality test. For this specific analysis, we excluded Plot 13, where we did not observe an upper layer (presumably due to a recent soil-consuming fire; Sleeter et al., 2017). Because some plots did not have a lower layer present, we conducted these analyses separately for three different plot categories: all plots (except plot 13); plots with only an upper layer observed; and plots with both upper and lower layers present. We also used the water table depth CDFs to identify the percentile that coincided with the upper layer thickness for each subplot, and then assessed the distribution of these values for each subplot category. Last, we re-ran this CDF analysis for nine plots with existing water table data for at least 4.75 years (compared to the 2.5-year record) to extend inferences to longer time periods.

2.4 Objective 2: Comparing Upper and Lower Layer Properties

2.4.1 Soil Sampling

At one subplot per plot (the 0° azimuth location), soil samples were obtained from the 25^{th}, 50^{th} and 75^{th} depth percentiles of each observed layer based on characterized soil profiles (Section 2.3.1). If the observed layer was less than 40 cm thick, then only one sample at the layer midpoint (50^{th} percentile) was collected. Laboratory analyses for bulk density and hydraulic properties required intact, field-representative samples. For these samples, two separate sampling methods were needed due to differences in upper and lower soil structure and position. For all upper layer samples, a 5 cm diameter × 10 cm long (comprised of two 5 cm segments) Bulk Density Corer (AMS, Inc., American Falls, Idaho, USA) was used (Fig. 4C), which was determined most effective at obtaining a representative sample of the coarser upper layer. To avoid issues of compaction and disturbance we retained only the lower 5 cm segment. For lower layers, a Hand Core Sediment Sampler (Wildco®, Yulee, Florida, USA) was used to collect samples in 5 cm diameter × 25 cm long plastic tubes (Fig. 4D), which allowed us to access deeper soil positions. Once samples were collected, they were wrapped in plastic wrap and stored at 4°C until further processing and analysis. In the laboratory, lower layer tubes were cut down to 5 cm × 5 cm samples using a rotary hand saw to match the upper layer core dimensions. We also collected an unconsolidated sample at each sampling depth for destructive laboratory analyses (organic matter content, fiber content). In the upper layer, the unconsolidated sample was collected from the upper 5 cm segment within the bulk density sampler. In the lower soil layer, the unconsolidated sample was collected from just above the target 5 cm × 5 cm sample that was cut using a hand saw. Unconsolidated samples were stored in plastic bags until further processing and analysis.

2.4.2 Laboratory Analysis for Soil Physical and Hydraulic Properties

Collected soil samples were analyzed for the following physical properties: bulk density, organic matter content, and fiber content. Bulk density (g cm^{-3}) was determined using the intact samples after oven drying samples at 105°C for 24 hours (ASTM, 2008), following hydraulic property analysis (below). Organic matter and fiber content analyses were conducted using the unconsolidated grab samples, while the other properties were measured on the intact volumetric cores. Gravimetric moisture content (W; g/g) of the soils at time of sampling was calculated using the intact cores by (ASTM, 2020):

$$W = \frac{M_w - M_d}{M_d} x\ 100 \quad [1]$$

where M_w (g) is the field wet mass of the intact core sample and M_d (g) is the dry core sample mass. We then calculated the dry mass of each unconsolidated sample ($M_{d,s}$; g) using (ASTM, 2013):

$$M_{d,s} = \left[\frac{M_{w,s}}{(W + 100)}\right] x\ 100 \quad [2]$$

where $M_{w,s}$ (g) is the initial field mass of the unconsolidated sample.

Organic matter content was determined through soil mass loss on ignition at 380°C for 24 hours (ASTM, 2020). Fiber content was determined following ASTM (2013), where samples were first placed in a 250 mL beaker of 5% sodium hexametaphosphate for at least 15 hours and then stirred at 240 r min^{-1} for 10 min. This sample solution was poured over a 100-mesh sieve and washed with distilled deionized water until the water passing through the sieve ran clear. The sieve was then placed in a shallow tank of 2% HCl solution for at least 10 minutes and washed again with distilled deionized water. After washing, any large mineral grains and pieces of plant material (e.g., roots or wood) greater than 20 mm were removed. The remaining sample was then washed onto pre-weighed filter paper and placed in a drying oven at 105°C for 24 hours. Fiber content was determined by taking the dry mass of the fibers divided by the dry mass of the soil sample.

To determine hydraulic properties for each intact soil sample, we developed moisture release curves (MRCs) to quantify the relationship between soil water content and matric potential (expressed here as a positive tension) (Klute, 1986). We constructed MRCs for each sample by combining tension table approaches (Leamer and Shaw, 1941) for low tensions (1.5, 3, 4.5 and 6 kPa) and pressure plate approaches (Dane and Hopmans, 2002; ASTM International, 2016) for higher tensions (33 and 100 kPa).

The tension table apparatus (Fig. 5) used was designed to the specifications of Leamer and Shaw (1941). Intact soil core samples (5 cm × 5 cm) were saturated for 24 hours, weighed, and placed onto the tension table. Tensions were generated by adjusting the height of the leveling device (E) relative to the middle of the soil cores (G). Four tensions (1.5, 3, 4.5 and 6 kPa) were applied in increasing order. For each tension, samples were allowed to equilibrate for 24 hours on the tension table, weighed, and then re-saturated to repeat the process for the following tension.

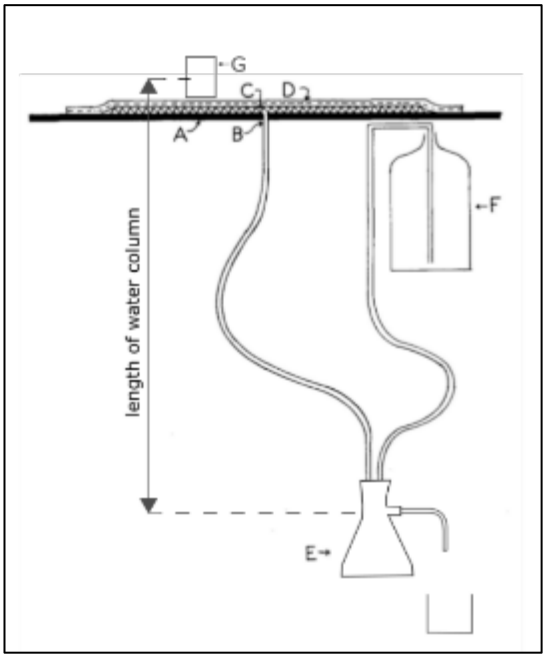

Figure 5: Diagram of the tension table used (redrawn from Leamer and Shaw, 1941): (A) wood base, (B) pipe nipple, (C) plastic mesh, (D) blotter paper, (E) leveling device, (F) water supply, and (G) soil sample. Used with permission from Trevor Amestoy, Virginia Tech Institute for Critical Technology and Applied Science, Research Undergraduate Fellow.

For tensions greater than 10 kPa, the pressure plate extraction method (Dane and Hopmans, 2002; ASTM International, 2016) was used to induce tensions. Using the same intact core samples from the tension table experiment, samples were saturated for 24 hours, weighed and placed on a ceramic plate (10 kPa rated plate) within the pressure chamber. Two pressures (33 and 100 kPa) were applied in increasing order. After samples reached equilibration (i.e., water no longer drained from the sample under the given tension), they were removed from the chamber, weighed and re-saturated for the following pressure application. Following the final pressure, samples were oven-dried at 105°C for 24 hours and M_d was determined.

For each tension applied (via both tension table and pressure plate methods), volumetric water content (VWC; g/cm^3) was determined using:

$$\theta(h) = \left(\frac{M_h - M_d}{V_t}\right) x\ 100 \qquad [3]$$

where $\theta(h)$ is VWC at a measured tension (h), M_h (g) is the mass of the sample at the measured tension, and V_t (cm^3) is the total sample volume.

The total porosity, ϕ, of each sample was calculated as the percentage of total volume filled by volume of water at saturation and thus equal to VWC at saturation (θ_s):

$$\phi = \frac{M_s - M_d}{V_t} \qquad [4]$$

A variation of the Brooks and Corey (1964) model for water retention was used to develop MRCs using determined VWC at each applied tension. The function is reduced to:

$$\theta(h) = (\theta_s + \theta_r) * \left(\frac{h_b}{h}\right)^{\frac{(\eta-2)}{3}+\theta_r} \qquad [5]$$

where parameters h_b (bubbling pressure), η (pore size index) and θ_r (residual water content) were optimized, minimizing the sum of squared residuals.

From the MRCS, a suite of hydraulic properties was derived including microporosity, macroporosity, plant available water content, specific yield, field capacity, and soil capillary length. Macroporosity is defined as the proportion of pores that drain under gravity and are ca. > 80 μm (Brady and Weil, 2010). Using the Young-Laplace equation, we solved for pore radius (r) of drained pores at MRC-modeled tensions (h):

$$r = \frac{-2\gamma(cos\alpha)}{\rho_w g h} \qquad [6]$$

where γ is surface tension, α is contact angle, ρ_w is the density of water, and g is gravity. The h = 15 cm tension equated to an approximate pore radius of 95 μm, so in this study we used that tension to distinguish macropores ($r > 95$ μm) from micropores ($r \leq 95$ μm) (Luxmore, 1981). Macroporosity (ϕ_m) as a percentage of total porosity was then calculated using modeled VWC loss at h =15 (θ_{15}):

$$\phi_m = \frac{\theta_{15}}{\phi} x\ 100 \qquad [7]$$

Microporosity as a percentage of total porosity was then determined by subtracting the known macroporosity percentage from 100.

Plant available water (PAW) was determined as the difference in MRC-modeled VWCs between tensions representing field capacity (33 kPa; Romano and Santini, 2002) and permanent wilting point (1500 kPa; Brady and Weil, 2010) and was reported as a percentage. Specific yield, defined as the amount of water loss under gravity (33 kPa), was calculated as the difference between modeled VWCs at saturation and field capacity and also reported as a percentage (Romano and Santini, 2002). Capillary length (λ) (cm) was calculated using parameters h_b and η from the modeled MRCs using (Stewart and Abou Najm, 2018):

$$\lambda = h_b \eta / (1 - \eta) \qquad [8]$$

2.4.3 Comparisons Between Upper and Lower Soil Layer Properties

To evaluate differences in soil properties between layers, we conducted independent two-sample t-tests ($\alpha = 0.05$) on each observed property between the upper and lower layers. First, each data set was tested for normality using the Shapiro-Wilk test ($\alpha = 0.05$). If the data followed a normal distribution, an F-test was conducted to test for equal variances between the two data sets. If the variances were equal, then a two-sample student's t-test was performed. If the variances were unequal, a Welch's t-test was conducted instead. If the data sets were found to not follow a normal distribution, then a nonparametric Wilcoxon sum rank test was performed.

Depending on sample size, we also compared some properties (specifically bulk density, fiber content, organic matter and total porosity) among sampling locations within the upper layer using a one-way analysis of variance (ANOVA) ($\alpha = 0.05$). We tested ANOVA assumptions of normal distribution by using the Shapiro-Wilk ($\alpha = 0.05$) test on ANOVA residuals, and common variance using the Bartlett test of homogeneity ($\alpha = 0.05$). If the ANOVA did not meet one or both of the test assumptions, the Kruskal-Wallis rank sum test was used as a non-parametric alternative. Within-layer statistical tests were not conducted on the lower layer due to the low sample size at some of the sampling locations.

We also assessed relationships among all observed physical and hydraulic properties using two different analyses. First, we used a nonmetric multidimensional scaling (NMDS) in R (R Core Team, 2016), using 'metaMDS' function in the 'vegan' package (Oksanen et al., 2019). Soil property data were input as processed and then scaled to normalize using the Wisconsin double standardization. The analysis was conducted using the Bray-Curtis dissimilarity method, and a stress test was used to determine goodness-of-fit. The resulting property vectors were fit to the axes using the 'envfit' function to show each parameter's relationship in ordination space. Second, we explored correlations among all soil properties using a Spearman's rank correlation ($\alpha = 0.05$).

3. Results

3.1 Relating Upper Layer Thickness to Hydrologic Regime

Peat soil depth, horizon distribution, and hydrologic regime varied across the Great Dismal Swamp plot network (Fig. 6). Total peat soil depths ranged from 34 cm to 283 cm across all plots. Of the 16 plots sampled, eight had both upper and lower layers present whereas seven plots had only an upper layer present. Plot 13 was located in the fire scar where we only observed the lower layer likely because the upper layer was consumed in recent fires. Upper and lower layer thicknesses were variable across plots, ranging from thick upper layers with thin lower layers (e.g., Plot 9) to thin upper layers with thick lower layers (e.g., Plot 10). There was also variability in layer thicknesses among subplots within plots, which typically exceeded subplot variation in ground surface elevation, as seen by comparing error bars in Fig. 6. Plots experienced variable hydrologic regimes, ranging from very wet sites with daily water tables existing above the ground surface (i.e., inundated conditions) for much of the year (e.g., Plots 4 and 8), to dry sites with limited inundation (e.g., Plots 3 and 6), to sites with more variable water table regimes (e.g., Plots 9 and 10). Notably, water tables only crossed the bottom boundary of the upper layer in seven of our 16 plots: Plots 2, 3, 6, 7, 9, 10, 12.

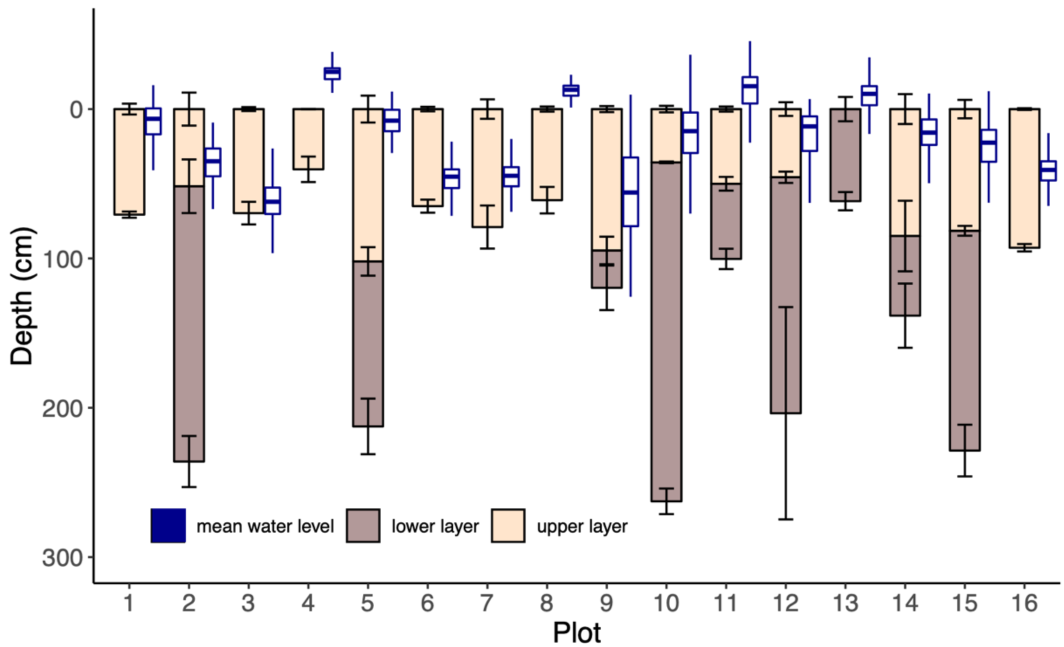

Figure 6: Mean ground surface elevation, total peat soil depth, and upper and lower layer thicknesses across subplots (n = 3) for each surveyed plot, with error bars (1.5 × standard deviation) denoting variation among subplots. Boxplot (blue) of 2.5-year continuous water table depths at each plot located to the right of each plot's soil profile.

We found significant correlations between several water table metrics and upper layer thickness, noting that analyses were conducted using three subplots per plot while excluding the recently burned plot 13 (Table 1). When pooling all subplots, there were significant and positive correlations for 25th, mean, median and 75th percentile water table depths, indicating that drier sites typically exhibited thicker upper layers. An example regression (Fig. 7) displays this general relationship (via mean water table depth), as well as the range of observed water table depths and upper layer thicknesses across all subplots. For plots with only an upper layer present, significant correlations were found for all water table depth metrics, except for standard deviation. However, there were no significant correlations for the eight plots with both an upper and lower soil layer present.

Table 1: Spearman's correlations between sub-plot upper layer thicknesses and water level depth metrics for: all plots; plots with only an upper soil layer present; and plots with both upper and lower layers present. Bold values denote significant correlations ($p < 0.05$).

	Water Table Metrics (m)					
	25th	Mean	Median	75th	95th	St. Dev.
All Plots (n = 45)	**0.43**	**0.44**	**0.46**	**0.41**	0.27	-0.16
Upper Only (n = 21)	**0.49**	**0.49**	**0.49**	**0.49**	**0.45**	0.35
Upper and Lower (n = 24)	0.33	0.29	0.31	0.16	-0.10	-0.39

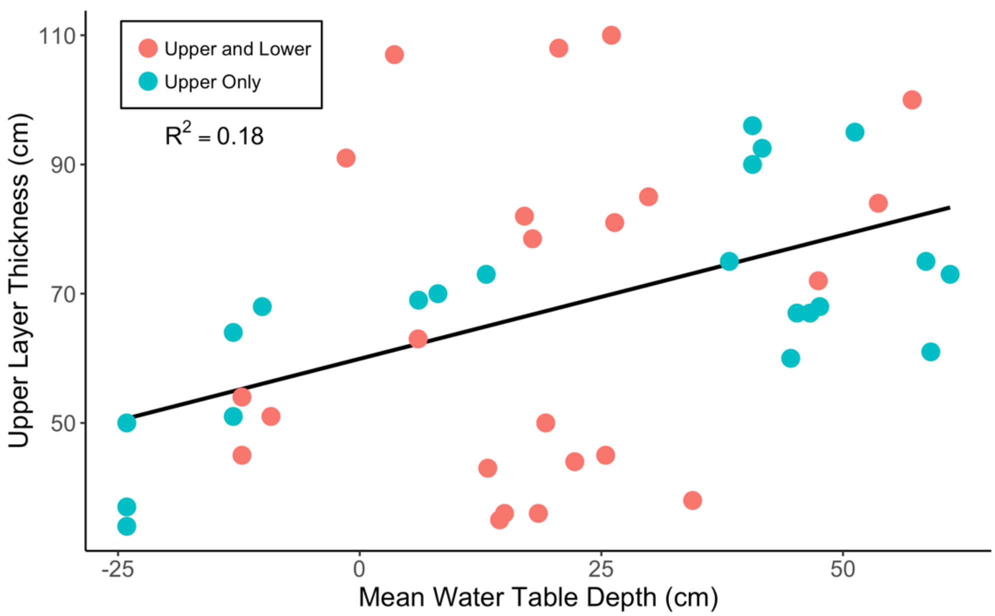

Figure 7: Upper soil layer depth versus mean water table depth for all subplots. Subplots with both upper and lower layers (n = 24) are shown in red, and subplots with only an upper layer (n = 21) are shown in blue. Linear regression statistics correspond to analysis of all plots.

Using water table depth CDFs, we also quantified the water table depth percentile that coincided with the upper layer bottom boundary at each subplot (an example of this analysis is presented in Figure 8). However, 26 subplots (out of a total of 45) never experienced a water table below the bottom boundary of the upper layer over the 2.5-year record (Fig. 6), precluding such an analysis for these subplots. For the remaining 19 subplots, the depths of intersection between water tables and layer boundaries corresponded to relatively deep water tables. For each pooled category (all plots, upper and lower, and upper layer only), the mean depths of intersection occurred at the 86th percentile of water table depth, whereas the median probability for each category ranged from the 87th (for plots with both upper and lower layers) to 92nd percentile (for plots with only an upper layer; Fig. 9). Only three subplots had upper layer boundaries occur at depths with water table probability values lower than the 80th percentile. Together, these results indicate that the bottom boundary of the upper layer occurred at extremely deep water tables (for 19 subplots) or below observed water tables (for 26 subplots) over the 2.5-year record. Lastly, we repeated this analysis for nine plots (27 subplots) with available water table data for 4.75 years and found similar results. For these subplots, 12 never experienced water tables below the bottom boundary of the upper layer, compared to 17 when assessing their 2.5-year record. For those that did, the upper layer bottom boundary occurred on average at the 90th water table depth percentile (data not shown), thus extending the general finding to longer time periods and more variable hydrologic regimes.

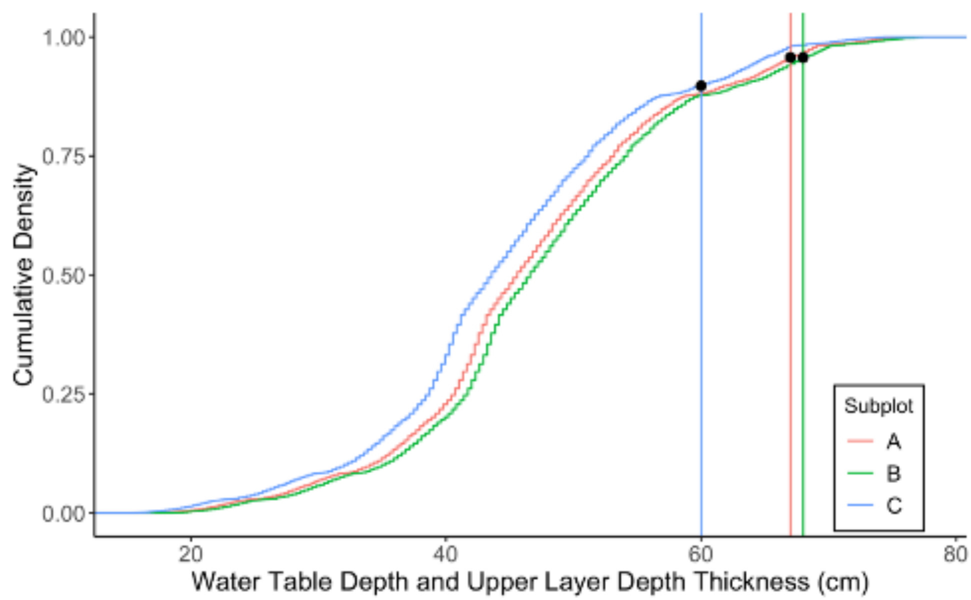

Figure 8: Example of a cumulative density function (CDF) at Plot 6 for subplot water table depths over the 2.5-year record. Subplot upper layer thicknesses are indicated by the vertical lines, showing that the bottom layer of the upper layer intersected water table depths representing the 96th (subplot A), 96th (subplot B), and 90th (subplot C) percentiles.

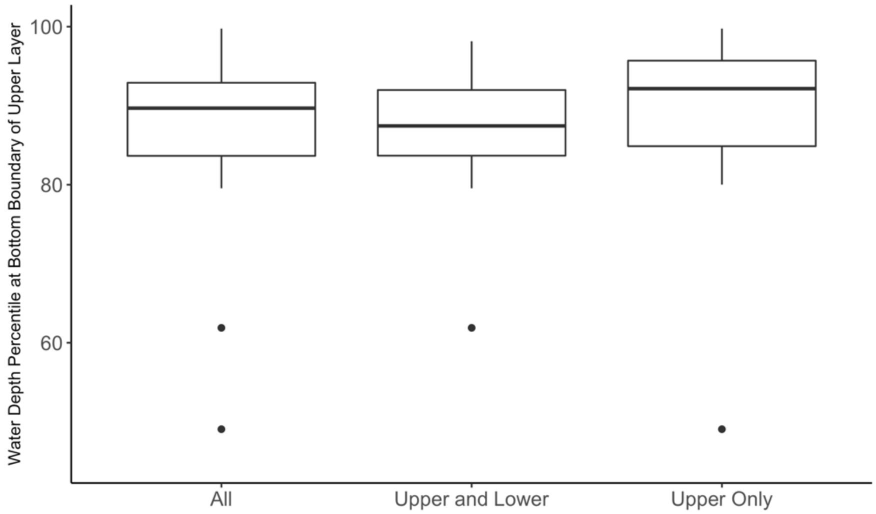

Figure 9: Distributions of water table depth percentiles that coincided with the upper layer bottom boundary for the 19 subplots (out of a total of 45) where observed water tables intersected the bottom boundary. Distributions are shown for the three plot categories: all plots, plots with upper and lower layers, and plots with only upper layers.

3.2 Soil Physical and Hydraulic Properties

We found significant differences in all of the quantified soil physical properties between the upper and lower layers (Fig. 10, left). The upper layer had a higher bulk density, with a mean of 0.17 g/cm^3 (0.06 g/cm^3 – 0.26 g/cm^3), than the lower layer (mean = 0.11 g/cm^3; range 0.07 g/cm^3 – 0.16 g/cm^3). We also found a lower percentage of organic matter in the upper layer (mean = 89.6%; range = 65.7% – 99.9%) compared to the lower layer (mean = 93.3%, range = 49.4% – 97.7%). Similarly, fiber content was lower in the upper layer (upper layer mean = 11.3% vs. lower layer mean = 16.7%). Property variation among sampling locations within each layer was far less than that between layers (Fig. 10, right). Indeed, in the upper layer, we found no significant differences in physical property values for within-layer sampling locations, further indicating distinct differences in layer properties as opposed to gradients along the soil profile. We note, however, that limited sample size precluded within-layer statistical comparisons for lower layer samples.

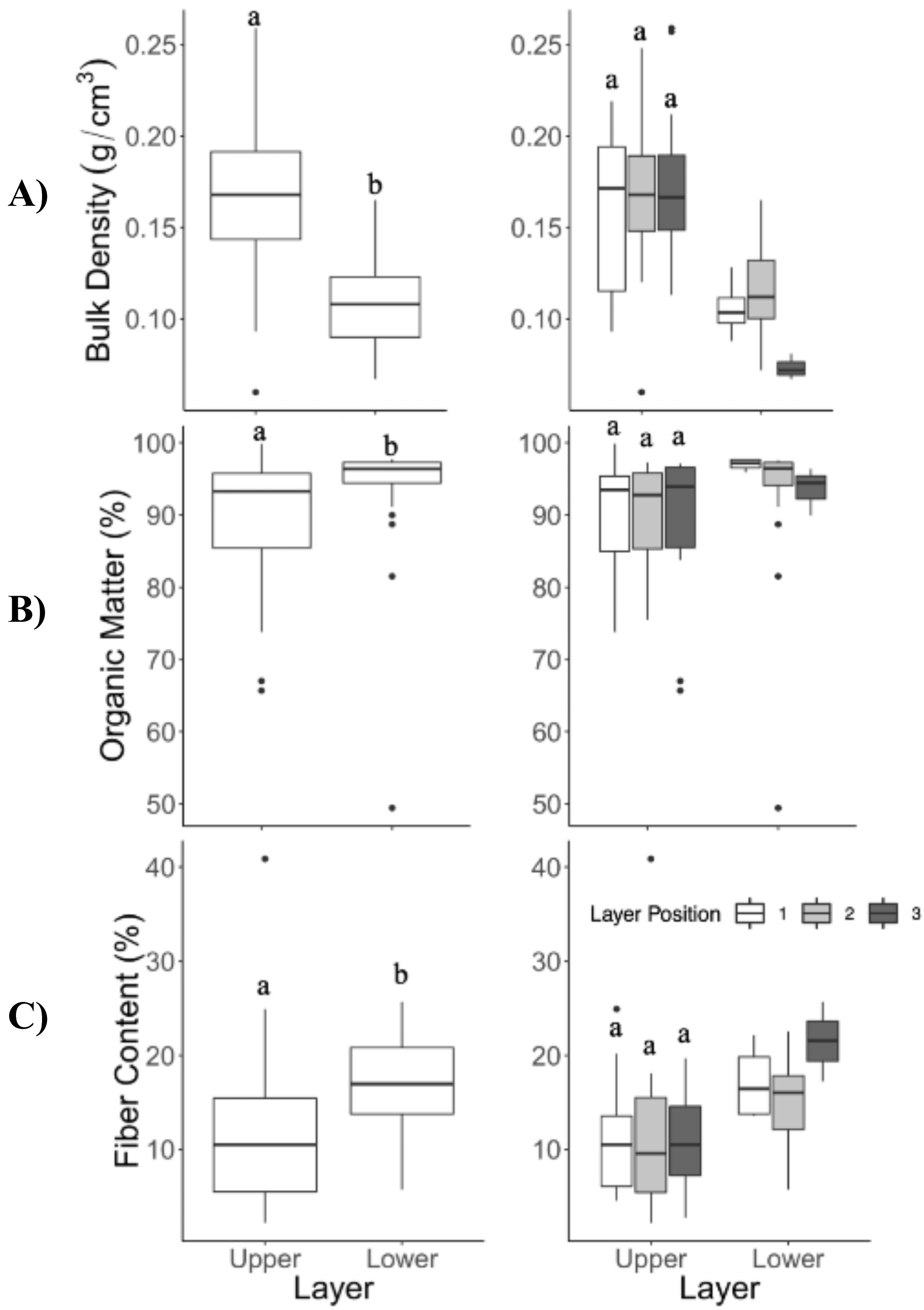

Figure 10: Distributions for peat (A) bulk density, (B) organic matter, and (C) fiber content between layers (left) and within layers (right). Pairwise comparisons, denoted by letters, were significant ($p < 0.01$) between layers. ANOVA results, denoted by letters, were not significant within layers ($p < 0.01$)

Constructed moisture release curves (MRCs) (n = 43) revealed generally lower water holding capacities in upper layers than lower layers. As an example, Figure 11 demonstrates lower VWCs in the upper layer across all tensions and that the upper layer also drained more rapidly (i.e., declines in VWC) with increasing tension, particularly at lower tension values.

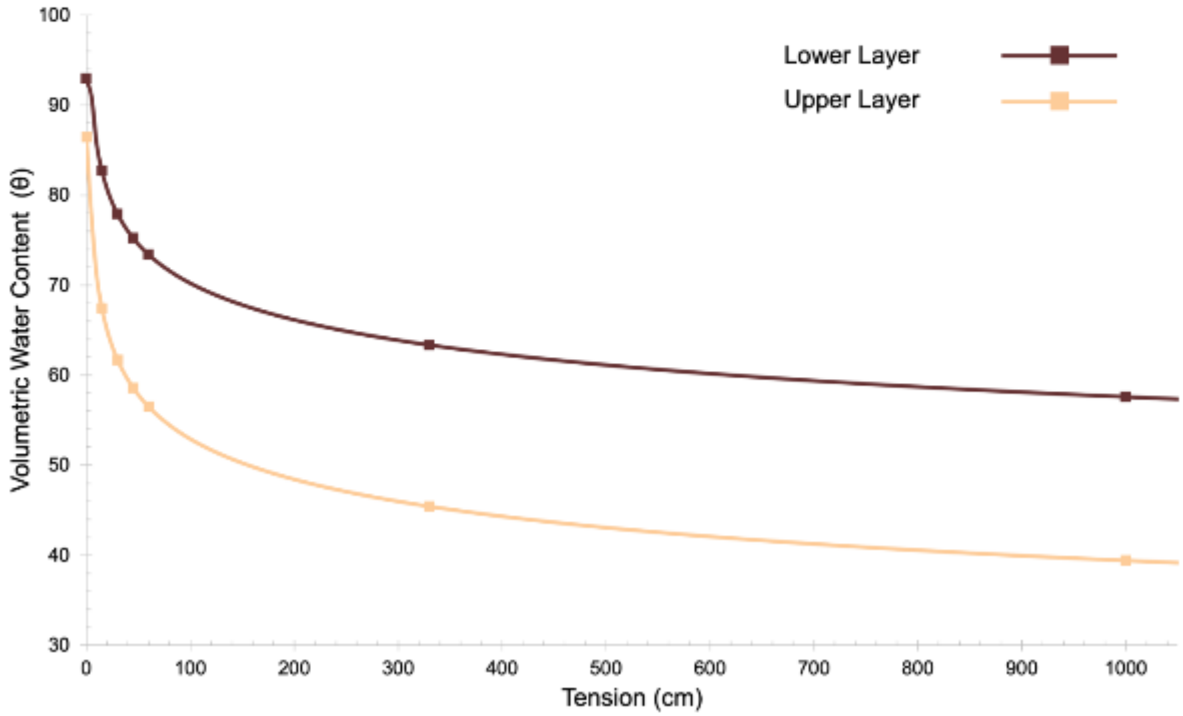

Figure 11: Moisture release curves (MRCs) generated from the Brooks and Corey (1964) water retention model for plot 11. The light line represents an MRC from the upper soil layer, and the dark line represents an MRC from the lower soil layer. The lower layer held more water at saturation (tension = 0 cm) and retained more water over the same tensions than the upper layer. The example here is consistent with findings from all other constructed MRCs.

MRCs also yielded specific soil hydraulic properties to further explore water retention differences between upper and lower soil layers. We found lower total porosities in the upper soil layer, ranging from 63.0% to 93.0% (mean = 83.3%), compared to the lower layer (mean = 93.2%, range = 78.0% – 101%) (Fig. 12A). Porosity values over 100% are attributed to sampling error when calculating the volume of the sample core. We also analyzed within-layer variability of total porosity in the upper layer and found no significant differences among sampling locations (Appendix, Fig. 15); sample size precluded such statistical comparisons for the lower layer sampling locations. When evaluating pore size structure, characterized by microporosity and macroporosity, we found a significantly higher proportion of macropores in the upper layer (mean = 30.9%, range = 11.5% – 63.0%) compared to lower layers (mean = 17.2%, range = 8.8% – 31.8%) (Fig. 12B). Consequently, microporosity was lower in upper layers (mean of 69.1% in upper layers versus 82.8% in lower layers), indicating lower moisture retention capacity. For the remaining quantified hydraulic properties, we found significant differences between layers in plant available water (PAW), capillary length, and field capacity, but not for specific yield (Table 2).

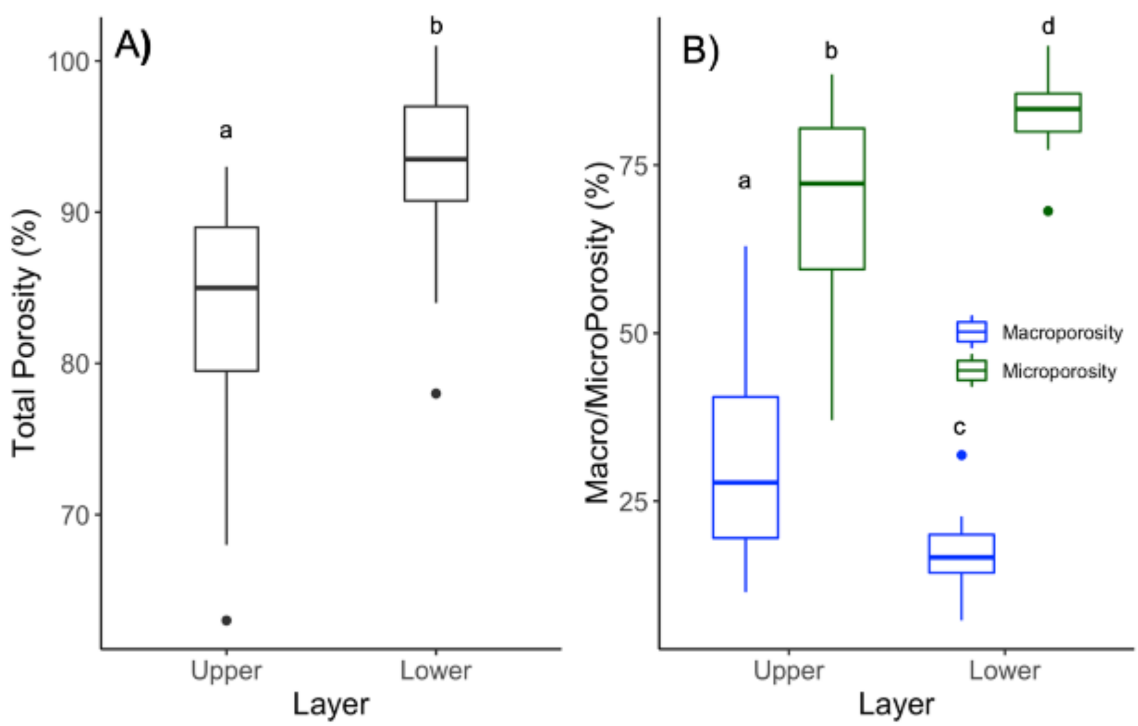

Figure 12: Distribution of (A) total porosity and (B) macroporosity (blue) and microporosity (green) between soil layers. Pairwise comparisons, denoted by letters, for total porosity, microporosity and macroporosity were significant ($p < 0.01$).

Table 2: Sample size (n), mean, and standard deviation (sd) of soil hydraulic properties for upper and lower soil layers, along with *p*-values from pairwise comparisons.

		Upper		Lower	
	n	mean (sd)	n	mean (sd)	p-value
Total Porosity (%)	27	83.3 (7.4)	16	93.2 (6.1)	<0.01
Microporosity (%)	27	69.1 (13.2)	16	82.8 (5.9)	<0.01
Macroporosity (%)	27	30.9 (13.2)	16	17.2 (5.9)	<0.01
Plant Available Water (%)	27	12.5 (3.9)	16	18.4 (3.0)	<0.01
Specific Yield (%)	27	40.1 (7.0)	16	39.1 (8.4)	0.69
Capillary Length (λ , cm)	27	1.7 (2.3)	16	5.5 (3.3)	<0.01
Field Capacity (θ_{fc})	27	43.3 (10.6)	16	54.1 (9.4)	<0.01

The nonmetric multidimensional scaling analysis (NMDS) using physical and hydraulic soil properties resulted in a two-dimensional solution with a stress of 0.07 (Fig. 13, Table 3). Physical properties were largely described by Axis 2, with increasing bulk density opposing fiber content and organic matter content. Hydraulic properties were more described by Axis 1, where increasing water retention properties (i.e., capillary length, PAW, and microporosity) opposed macroporosity. The ordination shows grouping of upper and lower layers; however, this grouping reveals larger separation along Axis 1, which is largely described by hydraulic properties.

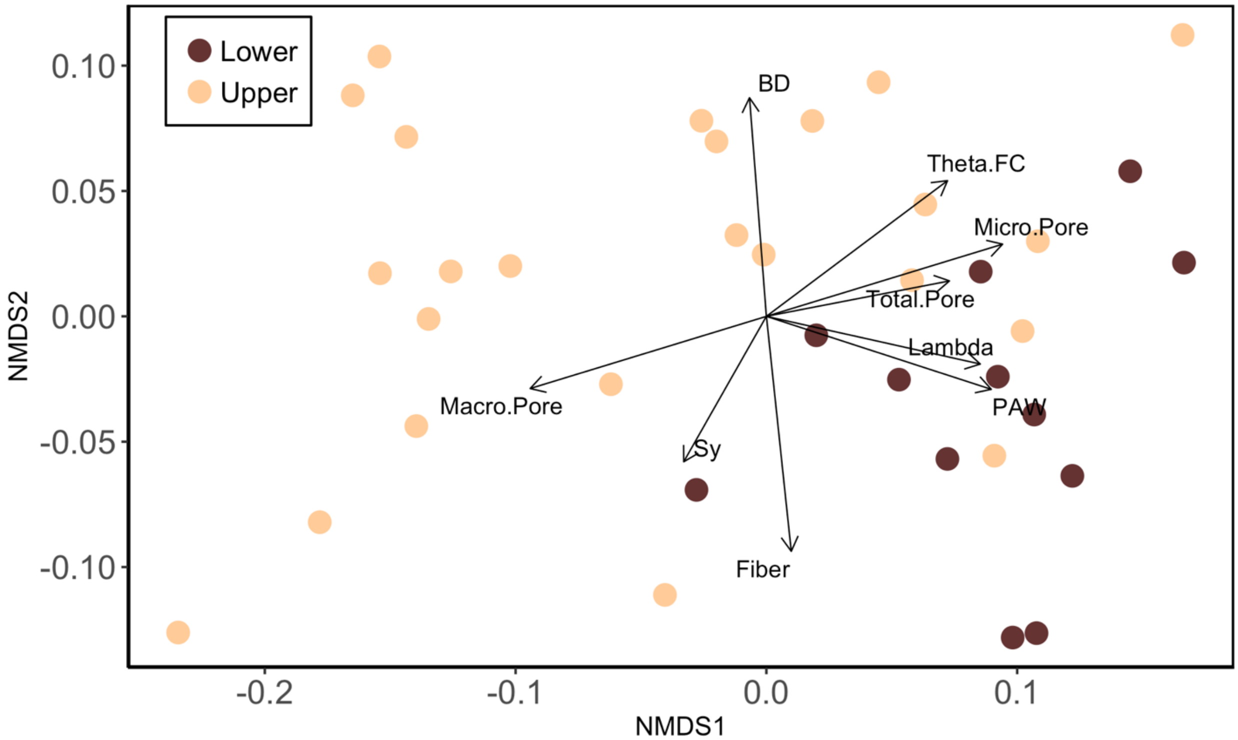

Figure 13: Nonmetric multidimensional scaling (NMDS) analysis with two dimensions to visualize peat property parameters with vectors present in the axes. Arrows show the direction of increasing parameter gradient, and lengths are proportional to the correlation between the parameter and ordination. BD = Bulk Density, Theta.FC = Field Capacity, Micro.Pore = Microporosity, Macro.Pore = Macroporosity, Total.Pore = Total Porosity, Lambda = Capillary Length, PAW = Plant Available Water, Fiber = Fiber Content, Sy = Specific Yield.

Table 3: Factor averages of soil properties in the NMDS axes. Columns Axis 1 and Axis 2 show correlation coefficients of soil properties with each axis and give direction to the vectors. R^2 values quantify the degree to which the ordination space affects the variable distribution, and is proportional to vector length. P-values show significance of soil properties on ordination of observations (points).

	Axis 1	Axis 2	R^2	P
Bulk Density	-0.08	0.99	0.76	<0.001
Organic Matter	-0.37	-0.93	0.11	0.06
Fiber Content	0.11	-0.99	0.89	<0.001
Total Porosity	0.98	0.19	0.55	<0.001
Microporosity	0.96	0.29	0.97	<0.001
Macroporosity	-0.96	-0.29	0.97	<0.001
Plant Available Water	0.95	-0.31	0.89	<0.001
Specific Yield	-0.49	-0.87	0.45	<0.001
Capillary Length (λ)	0.98	-0.22	0.76	<0.001
Field Capacity (θ_{fc})	0.80	0.60	0.81	<0.001

Consistent with findings from the NMDS analysis, we found significant correlations among physical soil properties, with negative correlations between bulk density and fiber content (Table 4). Similarly, there were significant negative correlations between macroporosity and several other hydraulic properties, including total porosity, microporosity, plant available water, capillary length and field capacity. However, there were no significant correlations between physical and hydraulic properties, indicating that variation in physical properties within and between layers does not explain observed variation in water retention properties.

Table 4: Spearman's correlation matrix of soil property variables. Bold values indicate a p-value of < 0.05. BD = Bulk Density, OM = Organic Matter, FC = Fiber Content, TP = Total Porosity, Micro = Microporosity, Macro = Macroporosity, PAW = Plant Available Water, S_y = Specific Yield, λ = Capillary Length, θ_{fc} = Field Capacity

	BD	OM	FC	TP	Micro	Macro	PAW	S_y	λ	θ_{fc}
BD	1									
OM	-0.30	1								
FC	**-0.80**	0.28	1							
TP	-0.16	0.11	0.17	1						
Micro	-0.05	0.11	0.10	**0.74**	1					
Macro	0.05	-0.11	-0.10	**-0.74**	**-1**	1				
PAW	-0.25	-0.09	0.26	**0.80**	**0.85**	**-0.85**	1			
S_y	-0.23	-0.28	0.20	-0.19	**-0.69**	**0.69**	-0.27	1		
λ	-0.24	-0.06	0.25	**0.71**	**0.90**	**-0.90**	**0.95**	**-0.43**	1	
θ_{fc}	0.12	0.23	-0.09	**0.76**	**0.93**	**-0.93**	**0.69**	**-0.73**	**0.72**	1

4. Discussion

In this work, we sought to explore hydrologic controls on upper layer thickness, contrast upper and lower layer soil properties, and relate these to implications for drained peatland restoration and management. To do so, we coupled continuous water level data with soil profile characterization and analyzed soil samples for their physical and hydraulic properties. Our findings highlight that the thickness of upper layers varies among and within plots and likely developed during periods of deep water tables, suggestive of past drainage effects as opposed to contemporary water level controls. We also found significant differences in properties of upper and lower soil layers, with lower moisture retention capacity in upper layers, and thus implications for soil moisture regimes and associated functions. Together, our findings will help inform restoration and water level management at GDS and our understanding of drained peatland soil-water interactions more broadly.

4.1 Hydrologic Controls on Upper Soil Layer Thickness

Hydrologic regime exerts strong controls on peat soil layer thicknesses and distributions by influencing decomposition rates within the soil profile. For example, in undisturbed peatlands, the mean summer water table influences the transition between the more aerobic, younger, and less decomposed upper layers and the persistently saturated, older, and more decomposed lower layers (Ingram, 1978; Clymo, 1984). However, peatland drainage can further increase the frequency (and depth) of aerobic conditions, permanently altering upper layer structure and properties (Schwärtzel et al., 2002; Gebhardt, 2009: Verry et al., 2011). Indeed, the USDA NRCS soil survey (Soil Survey Staff, 2020) details that after drainage at our study site, GDS, upper peat layers formed a weak subangular blocky structure. GDS experienced ditching and draining for ca. 200 years before the U.S. Fish and Wildlife Service began installing water control structures to raise water tables to their historical levels. Yet, the extent to which upper layer thicknesses respond to contemporary water levels remains largely unknown both at GDS and other restored, previously drained peatland systems.

We explored relationships between current water table regimes and upper soil layer thickness across 45 sampling points (15 plots, each with 3 subplots), capturing variation across spatial (ca. 45,000 ha) and temporal (2.5-year, sub-daily water levels) scales. When characterizing soil profiles, visual differences between upper and lower layers were clear, where upper layers were subangular blocky and coarse in texture, underlain by a more massive sapric lower layer. These observations are consistent with Soil Survey (2020) descriptions of an upper layer structure due to previous drainage. Moreover, upper layers appeared to be homogenous throughout their profile, with distinct and abrupt boundaries between upper and lower layers. This contrasts undisturbed peat profiles, where depth-dependent gradients in properties are apparent (Boelter, 1968; Ingram, 1978; Clymo, 1984), further supporting the notion that upper layer structure and depth resulted from altered hydrologic regimes.

Distinct upper and lower layers allowed us to clearly quantify upper layer thicknesses at each subplot and then relate those to measured water table regimes. We found some significant, albeit weak to moderate, relationships between upper layer thickness and several water table metrics (Table 1). However, the bottom boundary of the upper layer was generally much lower than the mean water table. This result again stands in contrast to undisturbed peat soils, where the mean summertime water table often serves as the dividing line between layers (Clymo, 1984). For example, in Figure 6 (highlighting Plots 5, 11, 14 and 15), we would expect to observe water tables near the transition between upper and lower layers, yet this did not occur over the course of the 2.5-year water level observational period. Further, we found that of our 45 subplots, only 19 experienced a (sub-daily) water table below the upper soil layer (Fig. 6), and for those that did, only extremely deep water table conditions (mean water table probability = 86^{th} percentile) coincided with the bottom boundary of the upper layer (Fig. 9). Furthermore, this finding remained the same when extending water table records to 4.75 years, indicating that the majority of contemporary water table depths occur above the bottom boundary of the upper layer.

The potential implications of our findings are twofold. First, as the water table largely controls peat decomposition and resulting layer formation (Ingram, 1978; Clymo, 1984), there is an expected relationship between upper layer depth and water table depth, similar to observations of drained and undrained peatlands made by Whittington and Price (2006). Thus, the observation that upper peats at GDS are typically deeper than most (if not all) recently observed water tables suggests that upper layer thicknesses are an artifact of historical drainage as opposed to contemporary water tables. Second, our findings suggest that the resulting upper layer is persistent with little recovery under wetter conditions. In support, Peng et al. (2007) and Peng and Horn (2007) documented irreversible structural changes to organic soils during drying and wetting cycles, detailing pronounced shrinkage and associated increases in large pores during drying but only minor swelling and recovery upon rewetting. Similarly, Gebhardt et al. (2009 and 2012) documented irreversible shrinkage in peat soils, with permanent changes to their physical (increasing bulk density) and hydraulic (increasing hydraulic conductivities) properties. Consequently, water management efforts at GDS and other drained peatlands should consider potential and persistent changes in upper soil properties that may impact soil moisture regimes and associated functions.

4.2 Differences in Soil Physical and Hydraulic Properties

We found significant differences in physical properties (bulk density, organic matter, and fiber content) between layers at GDS. Our findings are inconsistent with typical undrained peatland soil profiles, but instead are supportive of our field observations (i.e., distinct and coarse upper layer) and suggestive of consequences of drainage and increased aerobic conditions. Typically, we expect to find age- and depth-dependent gradients in soil properties, where bulk density increases and organic matter and fiber contents decrease with depth (Boelter, 1968) (Fig. 14A), driven by greater degrees of decomposition (Belyea and Clymo, 2001). However, we found the opposite at GDS, with lower fiber and organic matter contents and higher bulk densities in the upper layers (Fig. 14B). While upper layers in undisturbed peat soils also experience more frequent aerobic conditions than lower levels, they are less decomposed due to younger age (Clymo, 1984). Lower fiber content and organic matter in upper layers at GDS suggest drainage-induced increases in oxidation and decomposition that outweigh the effect of longer residence times in lower layers. As bulk density is strongly linked to degree of decomposition (Boelter, 1968), our findings further suggest that upper layer properties have been altered and reflect increased oxidation from historical drainage. As shown elsewhere, drained peats generally have higher bulk densities and lower organic matter content than their undisturbed reference peats (Kechavarzi et al., 2010; Leifeld et al., 2011), indicative of higher decomposition.

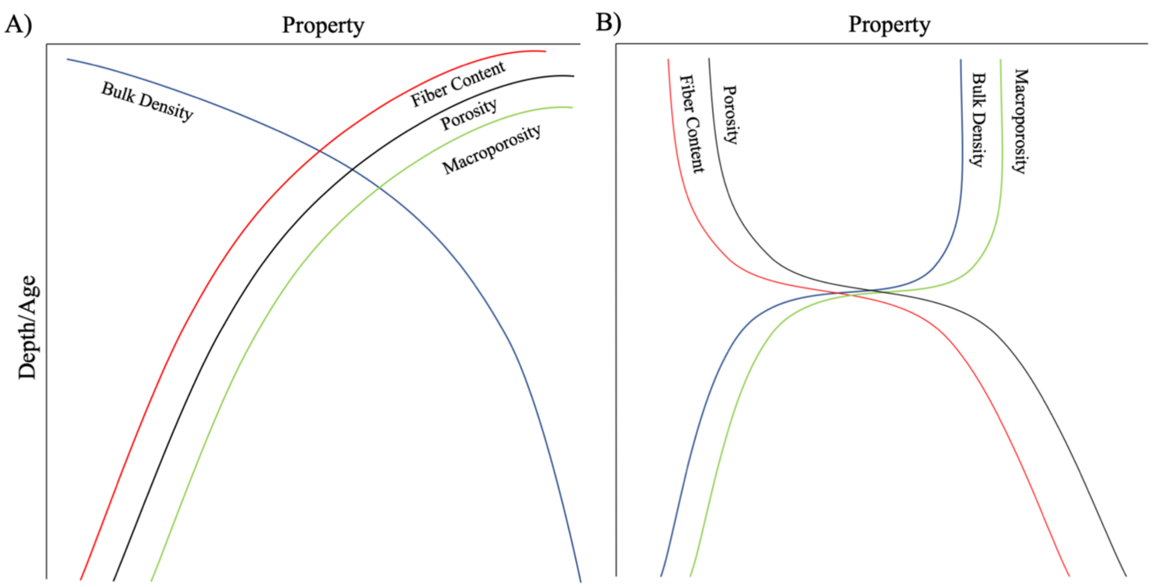

Figure 14: Conceptual models of A) undisturbed peat property profiles versus B) observed peat property profiles at GDS. Increased decomposition and soil shrinkage in upper layers as a result of historical drainage have altered typical depth/age relationships at GDS.

Notably, we also found a lack of the property gradients, especially in the upper layer, that typically characterize peat profiles. That is, there were no significant differences in physical properties among upper layer sampling positions (Fig. 10), indicating that the entire layer had been exposed to a similar set of environmental conditions (i.e. more frequent aerobic conditions). This contrasts typical peat profile gradients (Fig. 14A) and results in a new conceptualization characterizing soil profiles at GDS and likely other drained peatlands (Fig. 14B).

In addition to increased oxidation, peat soils can also experience irreversible shrinkage during intense drainage events, affecting soil hydraulic properties such as porosity and pore size distribution (Schwärtzel et al., 2002, Peng et al., 2007; Peng and Horn, 2007; Gebhardt et al., 2012). Concurrent with observed physical properties, we found significant differences in pore volume and pore size distribution between upper and lower layers. Specifically, we observed lower total porosities (Fig. 12a), and higher macroporosities and thus lower microporosity in upper layers (Fig. 12b), consistent with findings by Wallor et al. (2018). Under extreme and more frequent drying events, organic-rich soils can experience persistent shrinkage-induced changes to soil structure that decrease total pore volume, but result in an overall increase in macroporosity (Peng et al., 2007; Peng and Horn, 2007). These shrinkage-induced changes to pore structure can result in lower moisture retention capacity and further influence feedbacks to hydrologic regimes. Indeed, compared to lower layers, upper layers had significantly lower values for several MRC-derived metrics, including PAW and field capacity (Table 2), where increased macroporosity lowers overall moisture holding capacity (Holden and Burt, 2003). Our findings are also consistent with Wallor et al. (2018), showing that shrinkage reduces soil capillary length in upper soil layers.

We note, however, that higher macroporosities and associated hydraulic conductivities typically characterize the upper layer of undisturbed peat profiles (Clymo, 1984), but contend that shrinkage has resulted in further increases compared to undisturbed conditions (Gebhardt et al., 2009; Gebhardt et al., 2012). As support of shrinkage potential with drying, we analyzed our soil cores for saturated mass loss at each MRC tension point and found that lower layer samples lost ca. 11% of saturated mass over the entire range of tensions compared to ca. 6% from upper layers (Appendix, Table 5). Such saturated mass loss during drying is indicative of volume changes (i.e., shrinkage), and larger losses to lower layer samples suggests that the upper layer has experienced more shrinkage prior to our MRC analysis. These findings are further supported by similar work conducted by Schwärtzel et al. (2002) and Wallor et al. (2018), both of whom found greater shrinkage in undisturbed peats than drained peats during MRC analysis.

Last, while degree of decomposition and associated changes in physical properties, namely bulk density, can also lead to changes in hydraulic properties (Boelter, 1968, Verry et al., 2011), we found that changes in soil structure (e.g., increased macroporosity) had the strongest effect on water retention. That is, through NMDS analysis we found that hydraulic properties were largely described by Axis 1, where increasing water retention properties opposed macroporosity (Fig. 13, Table 3). Further, upper and lower layers were generally grouped by Axis 1 (and thus hydraulic properties), and we found no correlations between physical and hydraulic properties (Table 4). In short, we suggest that both increased decomposition and shrinkage affect, and potentially in different ways, specific peat properties, but that untangling those influences remains a research challenge.

4.3 Consequences for Management

We found that as a consequence of historical drainage, a distinct upper soil layer was formed and may permanently exist across GDS. This upper layer exhibits distinct physical and hydraulic properties that are uniform with depth and may have important implications for ecosystem functions. GDS uses water control structures in an effort to restore historical water levels and achieve management goals, such as restoring forest communities, reducing soil subsidence and oxidation, and decreasing fire vulnerability (Wurster et al., 2016). Our findings highlight important considerations for such efforts, namely to recognize the potential influence of altered upper layer properties on soil moisture regimes and associated management goals.

Lowered water tables and altered peat soil properties in drained peatlands have increased the frequency and extent of smoldering peat fires (Turetsky et al., 2014), which are largely controlled by soil moisture regimes (Frandsen, 1997; Schulte et al., 2019a). Our work highlights the vulnerability of upper soil layers to drying even under relatively low tensions (and thus water table depths), emphasizing the need to manage water levels at GDS to reduce fire risk. While the goal of USFWS is to re-wet GDS to historical water levels, these findings suggest that even higher water tables may have to be maintained to achieve sufficient soil moistures to reduce fire vulnerability. Typically, peatlands are protected from deep burning peat fires as the soil-moisture feedbacks that develop with depth and decomposition maintain conditions that are too wet to sustain deep smoldering (Turetsky et al., 2014). However, our observation of a homogenous upper, and often thick, layer with lower moisture retention likely increases the probability of smoldering, subsurface peat fires. Moreover, increased bulk densities associated with soil shrinkage, implies that if the upper layer does ignite, more organic material per unit volume is going to be consumed when compared to undrained peatland fires, highlighting an important consequence for carbon emissions. Indeed, two large fires recently burned at GDS, the 2008 South One Fire and the 2011 Lateral West Fire, which burned over 2,400 ha each and together consumed approximately 1.7 Tg of carbon (Sleeter et al., 2017). Soil moisture thresholds are often used for smoldering peat fire prediction, typically relying on weather variables to estimate surface soil moistures (F. Wurster, GDS Hydrologist, personal communication). As demonstrated by Schulte et al. (2019a), however, constructed MRCs and *in situ* water table data can be used for alternative, and likely more informed, surface soil moisture predictions. Our work extends this possibility by constructing different MRCs with depth, providing a framework for predictions of both surface ignition and burn depths from water table data.

Drainage at GDS has increased peat oxidation and subsidence, with important consequences for carbon storage and emissions (Drexler et al., 2017). As peat accumulation is the defining and functionally important characteristic of peatland systems, reducing subsidence and increasing accumulation is considered the most important aspect of restoration practice (Chimmer et al., 2016). Concurrent with conclusions about water management when considering fire vulnerability, our findings suggest that a higher than typical water table may be needed to achieve target surface moisture regimes in order to accumulate peat. Coupling derived MRCs with available water table models, such as the one developed by Eggleston et al. (2018), offers a potentially useful tool for informing decisions regarding water control management to maintain desired soil moisture regimes and enhance peat accumulation.

Vegetation composition change as a result of drainage at GDS and other peatlands has also been well documented. At GDS, communities have shifted from a mosaic of obligate wetland species to a more homogenous community dominated by facultative species, particularly red maple (Whitehead, 1972; Atkinson et al., 2003). Raising water tables to exclude facultative species can be effective (Vann and Megonigal, 2002) and indeed is a primary goal of current water level management at GDS. To that end, Schulte et al. (2019b) documented decreases in maple importance with increased wetness at GDS, indicating that higher water tables may help reduce red maple dominance and enable regeneration of more obligate wetland species. While some sites at GDS may be currently wet enough to support obligate species growth, our work shows that the ability for upper soil layers to rapidly dry likely allows aerobic conditions to persist at some times of the year and further support red maple dominance. Again, this may suggest a need to maintain water levels even higher than previous regimes, while also incorporating additional restoration efforts such as plantings and selective cuttings (Joosten and Clark, 2002; Quinty and Rochefort, 2003; Chimmer et al. 2016).

Lastly, the ultimate goal of peatland restoration is for peat formation to resume, often through encouraging the growth of peat-forming species like *Sphagnum* spp. (Gorham and Rochefort, 2003). *Sphagnum* is characterized by its moisture retention abilities, hence why it is recognized as a key building block of peatlands (Rochefort, 2000). Slowly, as new peat forms, positive ecohydrological feedbacks can establish, further enhancing peat formation (Rochefort, 2000). *Sphagnum* regeneration may be important at places like GDS because peat shrinkage via drainage is often permanent regardless of re-wetting efforts (Gebhardt et al., 2009). Thus, restoration at GDS and other drained peatlands may result in a soil profile that has an active *Sphagnum* surface layer underlain by newly formed "undisturbed" peat, but where the relic drained upper layer remains as a buried horizon. However, as peat growth and accumulation rates are extremely slow, estimated to be about 1 m every 1,000 to 2,000 years (Clymo, 1991), this now buried layer may remain close to surface; the extent to which it may act to disrupt soil moisture profiles and even act as a subsurface conduit for smoldering fire remains largely unknown.

4.4 Conclusions and Future Work

Our work highlights the consequences of drainage on organic soils in a temperate forested peatland. We sought to explore hydrologic controls on soil layer distributions and differences in their physical and hydraulic properties. Our work: i) suggests that altered peat properties resulted from past drainage with little recovery under wetter conditions and ii) documents consequences of both oxidation and soil shrinkage on hydraulic properties, with implications for contemporary soil moisture regimes and associated ecosystem functions.

Our work points to management and research needs at GDS and drained peatlands globally. First, managers could integrate MRC-derived hydraulic properties and water table data to predict soil moisture profiles over time and space. Such predictions could guide water level management to accomplish restoration goals, like increased carbon sequestration or specific vegetation composition. Further, soil moisture models could contribute to fire prediction efforts by integrating soil moisture burn thresholds (Schulte et al., 2019b) to predict both ignition probability and potential burn depths. Additionally, long term studies of peat properties are needed to assess drained peat response to hydrologic restoration (i.e., if they recover or remain buried under new peat accumulation). Last, we focused on a temperate, forested peatland with a specific type of organic soil, which may not be representative of other peatlands. This highlights the need for similar work to be conducted across the diversity of peatland systems, from boreal to tropical peatlands, to understand how differences in peat characteristics can influence their response to drainage and subsequent restoration.

5. Literature Cited

Atkinson, R. B., J. W. DeBerry, D. T. Loomis, E. R. Crawford, R. T. Belcher, D. A. Brown, and J. E. Perry. (2003). Water Tables in Atlantic White Cedar Swamps: Implications for Restoration. In *Atlantic White Cedar Restoration Ecology and Management, Proceedings of a Symposium. Christopher Newport University, Newport News*, 137–150.

ASTM International. (2008). ASTM D4531-86: Standard Test Methods for Bulk Density of Peat and Peat Products. West Conshohocken, PA: ASTM International.

ASTM International. (2013). ASTM D1997-13: Standard Test Method for Laboratory Determination of Fiber Content of Peat Samples by Dry Mass. West Conshohocken, PA: ASTM International.

ASTM International. (2016). ASTM D6836-16: Standard Test Methods for Determination of the Soil Water Characteristic Curve for Desorption Using Hanging Column, Pressure Extractor, Chilled Mirror Hygrometer, or Centrifuge. West Conshohocken, PA: ASTM International

ASTM International. (2020). ASTM D2974-20: Standard Test Methods for Determining the Water (Moisture) Content, Ash Content, and Organic Material of Peat and Other Organic Soils. West Conshohocken, PA: ASTM International

Belyea, L. R., & Clymo, R. S. (2001). Feedback control of the rate of peat formation. *Proceedings of the Royal Society of London. Series B: Biological Sciences*, *268*(1473), 1315–1321. doi: 10.1098/rspb.2001.1665

Boelter, DH. (1968). Important physical properties of peat material. *Proceedings of the Third International Peat Congress, 150-156.*

Bonn, A., Allott, T., Evans, M., Joosten, H., & Stoneman, R. (2016). Peatland restoration and ecosystem services: an introduction. *Peatland Restoration and Ecosystem Services*, 1–16. doi: 10.1017/cbo9781139177788.002

Brady, Nyle C., and Ray R. Weil. (2010). *Elements of the Nature and Properties of Soils*. 3rd ed., Pearson Educational International

Bridgham, S. D., Pastor, J., Janssens, J. A., Chapin, C., & Malterer, T. J. (1996). Multiple limiting gradients in peatlands: A call for a new paradigm. *Wetlands*, *16*(1), 45–65. doi: 10.1007/bf03160645

Brooks, R.H., & Corey, A.T. (1964). Hydraulic properties of porous media and their relation to drainage design. *Transactions of the ASAE*, *7*(1), 26–28. doi: 10.13031/2013.40684

Chimner, R. A., Cooper, D. J., Wurster, F. C., & Rochefort, L. (2016). An overview of peatland restoration in North America: where are we after 25 years? *Restoration Ecology*, *25*(2), 283–292. doi: 10.1111/rec.12434

Ciais, P., C. Sabine, G. Bala, L. Bopp, V. Brovkin, J. Canadell, A. Chhabra, R. DeFries, J. Galloway, M. Heimann, C. Jones, C. Le Quéré, R.B. Myneni, S. Piao and P. Thornton. (2013) Carbon and Other Biogeochemical Cycles. *Climate Change 2013: The Physical Science Basis. Contribution of Working Group I to the Fifth Assessment Report of the Intergovernmental Panel on Climate Change* [Stocker, T.F., D. Qin, G.-K. Plattner, M. Tignor, S.K. Allen, J. Boschung, A. Nauels, Y. Xia, V. Bex and P.M. Midgley (eds.)]. Cambridge University Press, Cambridge, United Kingdom and New York, NY, USA.

Clymo, R. S. (1984). The limits to peat bog growth. *Philosophical Transactions of the Royal Society of London. B, Biological Sciences*, *303*(1117), 605–654. doi: 10.1098/rstb.1984.0002

Clymo, R. S. (1991). Peat Growth. In *Quaternary Landscapes* (pp. 76–112).

Clymo, R. S., Turunen, J., & Tolonen, K. (1998). Carbon accumulation in peatland. *Oikos*, *81*(2), 368–388. doi: 10.2307/3547057

Dane, J.H. & Jan W. Hopmans. (2002). Soil Solution Phase: Laboratory. *Methods of Soil Analysis Part - 4 Physical Methods: SSSA Book Series - 5*, 675 – 720. Soil Science Society of America.

Dekker, L. W., & Ritsema, C. J. (1996). Variation in water content and wetting patterns in Dutch water repellent peaty clay and clayey peat soils. *Catena*, *28*(1-2), 89–105. doi: 10.1016/s0341-8162(96)00047-1

Drexler, J. Z., Fuller, C. C., Orlando, J., Salas, A., Wurster, F. C., & Duberstein, J. A. (2017). Estimation and uncertainty of recent carbon accumulation and vertical accretion in drained and undrained forested peatlands of the southeastern USA. *Journal of Geophysical Research: Biogeosciences*, *122*(10), 2563–2579. doi: 10.1002/2017jg003950

Eggleston, J. R., Decker, J. D., Finkelstein, J. S., Wurster, F. C., Misut, P. E., Sturtevant, L. P., & Speiran, G. K. (2018). Hydrologic conditions and simulation of groundwater and surface water in the Great Dismal Swamp of Virginia and North Carolina. *Scientific Investigations Report*. doi: 10.3133/sir20185056

FAO. (1985). *Irrigation Water Management: Training Manual No.2 – Elements of Topographic Surveying.* Land and Water Development Division. http://www.fao.org/tempref/agl/AGLW/fwm/Manual2.pdf

Frandsen, W. H. (1997). Ignition probability of organic soils. *Canadian Journal of Forest Research*, *27*(9), 1471–1477. doi: 10.1139/x97-106

Gebhardt, S., Fleige, H., & Horn, R. (2009). Shrinkage processes of a drained riparian peatland with subsidence morphology. *Journal of Soils and Sediments*, *10*(3), 484–493. doi: 10.1007/s11368-009-0130-9

Gebhardt, S., Fleige, H., & Horn, R. (2012). Anisotropic shrinkage of mineral and organic soils and its impact on soil hydraulic properties. *Soil and Tillage Research*, *125*, 96–104. doi: 10.1016/j.still.2012.06.017

Gorham, E. & Rochefort, L. (2003). Peatland restoration: A brief assessment with special reference to *Sphagnum* bogs. *Wetlands Ecology and Management, 11,* 109-119. doi: 10.1023/A:1022065723511

Holden, J., Evans, M. G., Burt, T. P., & Horton, M. (2006). Impact of land drainage on peatland hydrology. *Journal of Environmental Quality*, *35*(5), 1764–1778. doi: 10.2134/jeq2005.0477

Ingram, H. A. P. (1978). Soil Layers In Mires: Function And Terminology. *Journal of Soil Science*, *29*(2), 224–227. doi: 10.1111/j.1365-2389.1978.tb02053.x

IPCC. (2014). 2013 Supplement to the 2006 IPCC Guidelines for National Greenhouse Gas Inventories: Wetlands. Hiraishi, T., Krug, T., Tanabe, K., Srivastava, N., Baasansuren, J., Fukuda, M. and Troxler, T.G. (eds). Published: IPCC, Switzerland

Joosten, H., & Clarke, D. (2002). *Wise use of mires and peatlands: background and principles including a framework for decision-making*. Greifswald (Allemagne): International mire conservation group.

Kechavarzi, C., Dawson, Q., & Leeds-Harrison, P. (2010). Physical properties of low-lying agricultural peat soils in England. *Geoderma*, *154*(3-4), 196–202. doi: 10.1016/j.geoderma.2009.08.018

Klute, A. (1986). Water Retention: Laboratory Methods. *SSSA Book Series Methods of Soil Analysis: Part 1—Physical and Mineralogical Methods* doi:10.2136/sssabookser5.1.2ed.c26.

Kolka, R., Bridgham, S. D., & Ping, C.-L. (2016). Soils of Peatlands: Histosols and Gelisols. In *Wetland Soils: Genesis, Hydrology, Landscapes and Classification* (2nd ed., pp. 277–309).

Lappalainen, E. (1996). General review on world peatland resources. *Global Peat Resources.* International Peat Society, Finland. 53-56.

Leamer, R. W., & Shaw, B. (1941). A simple apparatus for measuring noncapillary porosity on an extensive scale. *Agronomy Journal*, *33*(11), 1003. doi: https://doi.org/10.2134/agronj1941.00021962003300110005x

Leifeld, J., Müller, M., & Fuhrer, J. (2011). Peatland subsidence and carbon loss from drained temperate fens. *Soil Use and Management*, *27*(2), 170–176. doi: 10.1111/j.1475-2743.2011.00327.x

Levy, G. F. (1991). The vegetation of the Great Dismal Swamp: A review and an overview. *Virginia Journal of Science 42*(4), 411–418.

Luxmoore, R. J. (1981). Micro-, Meso-, and Macroporosity of Soil. *Soil Science Society of America Journal*, *45*(3), 671–672. doi: 10.2136/sssaj1981.03615995004500030051x

Martin-Ortega, J., Allott, T. E., Glenk, K., & Schaafsma, M. (2014). Valuing water quality improvements from peatland restoration: Evidence and challenges. *Ecosystem Services*, *9*, 34–43. doi: 10.1016/j.ecoser.2014.06.007

Minayeva, T., Bragg, O., & Sirin, A. (2016). Peatland biodiversity and its restoration. *Peatland Restoration and Ecosystem Services*, 44–62. doi: 10.1017/cbo9781139177788.004

Mitsch, W. J., & Gosselink, J. G. (2007). *Wetlands*. Hoboken, NJ: Wiley.

Oksanen, J, F. G. Blanchet, M. Friendly, R. Kindt, P. Legendre, D. McGlinn, P. Minchin. (2019). *Vegan: Community Ecology Package* (version 2.5-6).

Osborn, C.C. (1919). Peat in the Dismal Swamp, Virginia and North Carolina. *Contribution to Economic Geology.*

Page, S. E., Rieley, J. O., & Banks, C. J. (2011). Global and regional importance of the tropical peatland carbon pool. *Global Change Biology*, *17*(2), 798–818. doi: 10.1111/j.1365-2486.2010.02279.x

Päivänen, J. (1982). Physical properties of peat samples in relation to shrinkage upon drying. *Silva Fennica*, *16*(3). doi: 10.14214/sf.a15076

Peng, X., Horn, R., & Smucker, A. (2007). Pore shrinkage dependency of inorganic and organic soils on wetting and drying cycles. *Soil Science Society of America Journal*, *71*(4), 1095–1104. doi: 10.2136/sssaj2006.0156

Peng, X., & Horn, R. (2007). Anisotropic shrinkage and swelling of some organic and inorganic soils. *European Journal of Soil Science*, *58*(1), 98–107. doi: 10.1111/j.1365-2389.2006.00808.x

PRISM Climate Group, Oregon State University, http://prism.oregonstate.edu, created 25 Nov 2019.

Quinty, F., & Rochefort, L. (2003). *Peatland restoration guide*. St. Albert, AB: Canadian Sphagnum Peat Moss Association.

R Core Team (2016). R: A Language and Environment for Statistical Computing. Vienna, Austria: R Foundation for Statistical Computing.

Rein, G., Cleaver, N., Ashton, C., Pironi, P., & Torero, J. L. (2008). The severity of smouldering peat fires and damage to the forest soil. *Catena*, *74*(3), 304–309. doi: 10.1016/j.catena.2008.05.008

Rochefort, L. (2000). Sphagnum—A keystone genus in habitat restoration. *The Bryologist*, *103*(3), 503–508. doi: 10.1639/0007-2745(2000)103[0503:sakgih]2.0.co;2

Schulte, M. L., Mclaughlin, D. L., Wurster, F. C., Varner, J. M., Stewart, R. D., Aust, W. M., Gile, B. (2019a). Short- and long-term hydrologic controls on smouldering fire in wetland soils. *International Journal of Wildland Fire*, *28*(3), 177. doi: 10.1071/wf18086

Schulte, M. L., Mclaughlin, D. L., Wurster, F. C., Balentine, K., Speiran, G. K., Aust, W. M., Jones, C. N. (2019b). Linking ecosystem function and hydrologic regime to inform restoration of a forested peatland. *Journal of Environmental Management*, *233*, 342–351. doi: 10.1016/j.jenvman.2018.12.042

Schwärzel, K., Renger, M., Sauerbrey, R., & Wessolek, G. (2002). Soil physical characteristics of peat soils. *Journal of Plant Nutrition and Soil Science*, *165*(4), 479–486. doi: 10.1002/1522-2624(200208)165:4<479::aid-jpln479>3.0.co;2-8

Sleeter, R., Sleeter, B. M., Williams, B., Hogan, D., Hawbaker, T., & Zhu, Z. (2017). A carbon balance model for the Great Dismal Swamp ecosystem. *Carbon Balance and Management*, *12*(1). doi: 10.1186/s13021-017-0070-4

Soil Survey Staff. (2020). Natural Resource Conservation Service, United States Department of Agriculture. *Soil Series Classification Database*.

Soil Survey Staff. (2014). *Keys to Soil Taxonomy*, 12th ed. USDA-Natural Resources Conservation Service, Washington, DC.

Stewart, R. D., & Najm, M. R. A. (2018). A comprehensive model for single ring infiltration I: initial water content and soil hydraulic properties. *Soil Science Society of America Journal*, *82*(3), 548–557. doi: 10.2136/sssaj2017.09.0313

Turetsky, M. R., & Louis, V. L. S. (2006). Disturbance in Boreal Peatlands. *Ecological Studies Boreal Peatland Ecosystems*, 359–379. doi: 10.1007/978-3-540-31913-9_16

Turetsky, M. R., Benscoter, B., Page, S., Rein, G., Werf, G. R. V. D., & Watts, A. (2014). Global vulnerability of peatlands to fire and carbon loss. *Nature Geoscience*, *8*(1), 11–14. doi: 10.1038/ngeo2325

U.S. Fish and Wildlife Service (USFWS). (2006). *Great Dismal Swamp National Wildlife Refuge and Nansemond National Wildlife Refuge Final Comprehensive Conservation Plan.*

U.S. Geological Survey. (2016). National Water Information System, data available on World Wide Web (USGS Water Data for the Nation) https://waterdata.usgs.gov/nwis/gw

Vann, C., & Megonigal, J. (2002). Productivity responses of *Acer rubrum* and *Taxodium distichum* seedlings to elevated CO_2 and flooding. *Environmental Pollution*, *116*. doi: 10.1016/s0269-7491(01)00244-5

Verry, E. S., Boelter, D. H., Päivänen, J., Nichols, D. S., Malterer, T., & Gafni, A. (n.d.). Physical Properties of Organic Soils. In *Peatland Biogeochemistry and Watershed Hydrology at the Marcell Experimental Forest* (1st ed., pp. 135–176). doi: https://doi.org/10.1201/b10708

Vasilas, L. M., Hurt, G. W., & Berkowitz, J. F. (2017). *Field indicators of hydric soils in the United States: a guide for identifying and delineating hydric soils*. Washington, D.C.: United States Department of Agriculture, Natural Resources Conservation Service.

Wallor, E., Rosskopf, N., & Zeitz, J. (2018). Hydraulic properties of drained and cultivated fen soils part I - Horizon-based evaluation of van Genuchten parameters considering the state of moorsh-forming process. *Geoderma*, *313*, 69–81. doi: 10.1016/j.geoderma.2017.10.026

Whitehead, D. R. (1972). Developmental and environmental history of the Dismal Swamp. *Ecological Monographs*, *42*(3), 301–315. Doi: 10.2307/1942212

Whittington, P. N., & Price, J. S. (2006). The effects of water table draw-down (as a surrogate for climate change) on the hydrology of a fen peatland, Canada. *Hydrological Processes*, *20*(17), 3589–3600. Doi: 10.1002/hyp.6376

Wurster, F. C., Ward, S., & Pickens, C. (2016). Forested peatland management in southeast Virginia and northeast North Carolina, USA, *Proceedings of the 15th International Peat Congress,* Sarawak, Malaysia.

Xu, J., Morris, P. J., Liu, J., & Holden, J. (2018). PEATMAP: Refining estimates of global peatland distribution based on a meta-analysis. *Catena*, *160*, 134–140. Doi: 10.1016/j.catena.2017.09.010

Yu, Z., Loisel, J., Brosseau, D. P., Beilman, D. W., & Hunt, S. J. (2010). Global peatland dynamics since the Last Glacial Maximum. *Geophysical Research Letters*, *37*(13). Doi: 10.1029/2010gl043584

6.0 Appendix

Table 5: Mean percent change (with standard deviation, sd) in saturated mass loss following tensions for upper and lower soil layers. Cores were not saturated after the 100 kPa tension.

	Saturated Mass Loss (%)			
Tension (kPa)	Upper		Lower	
	n	mean (sd)	n	mean (sd)
1.5	27	0.87 (1.67)	16	1.36 (2.82)
3	27	1.58 (1.98)	16	2.25 (3.66)
4.5	27	2.26 (2.22)	16	3.44 (3.80)
6	27	3.37 (2.91)	16	3.24 (2.79)
33	27	5.96 (3.85)	16	11.45 (7.32)

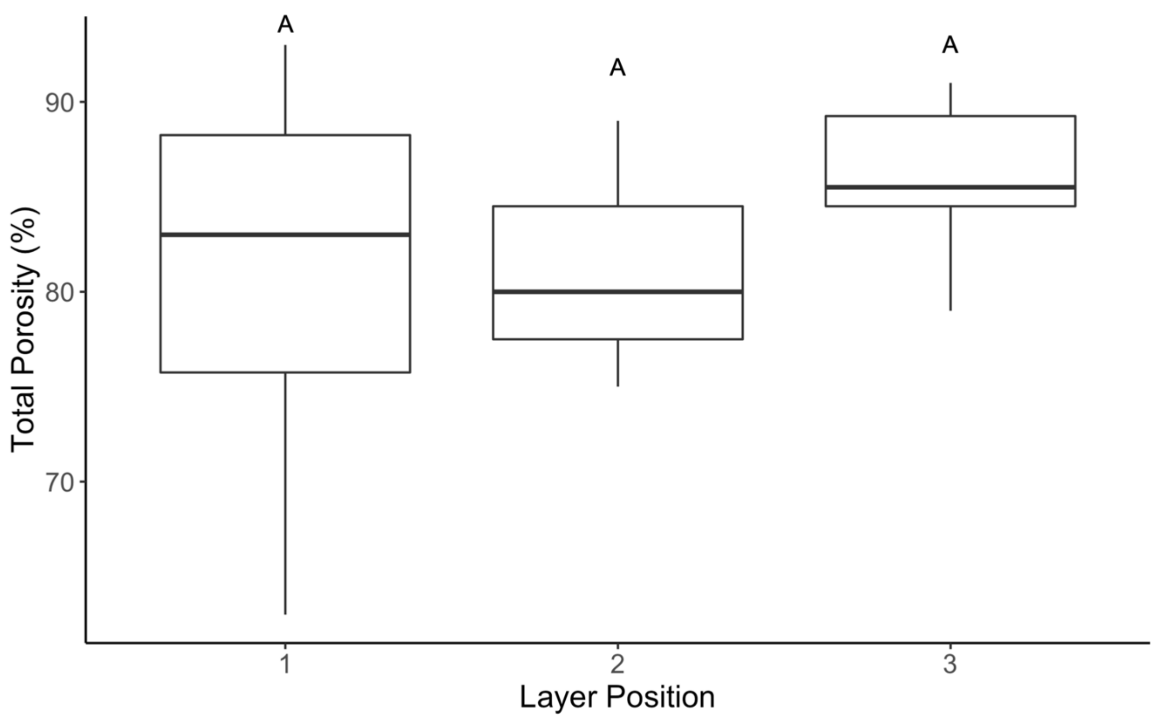

Figure 15: Distribution of total porosity within the upper layer at the upper (1), middle (2) and lower (3) sampling locations. ANOVA results, denoted by letters, were found not to be significant ($p < 0.05$).